

Design optimization with variable screening by interval-based sensitivity analysis

Qi Chang¹, Changcong Zhou², Matthias G.R. Faes³, Marcos A. Valdebenito⁴

Abstract: Design optimization problems are very common in engineering practice. Determining their solution may be challenging when many design variables are involved. A means to cope with such large number of design variables consists of first screening influential variables which drive the objective function the most. Then the optimization is carried out with respect to the influential variables while the other noninfluential variables are fixed at specific values. There is no doubt that an accurate identification of influential variables is crucial for high-dimensional optimization problems. In this paper, an interval-based sensitivity index is introduced to identify the influential variables and is theoretically compared with other two types of existing indices. The performance of these indices for dimensionality reduction in optimization is examined by means of a test function. Then, the proposed procedure for high-dimensional design optimization with variable screening is analyzed considering two illustrative examples. Then, the proposed strategy is applied to a practical engineering problem involving an aeronautical hydraulic pipeline. The results show that the interval sensitivity index is an effective tool and is superior to other two existing sensitivity indices for variable screening in design optimization.

Keywords: Optimization; Variable screening; Sensitivity; Interval; Hydraulic pipeline

¹ Ph.D. Candidate, Department of Engineering Mechanics, Northwestern Polytechnical University, Youyi West Road 127, 710072 Xi'an, China. Email: qichang@mail.nwpu.edu.cn

² Professor, Department of Engineering Mechanics, Northwestern Polytechnical University, Youyi West Road 127, 710072 Xi'an, China (corresponding author). Email: changcongzhou@nwpu.edu.cn

³ Professor, Chair for Reliability Engineering, TU Dortmund University, Leonhard-Euler-Strasse 5, 44227 Dortmund, Germany. Email: matthias/faes@tu-dortmund.de

⁴ Chief Engineer, Chair for Reliability Engineering, TU Dortmund University, Leonhard-Euler-Strasse 5, 44227 Dortmund, Germany. Email: marcos.valdebenito@tu-dortmund.de

22 **Introduction**

23 In engineering practice, a design optimization problem involves improving a predefined
24 performance measure by selecting input variables of the considered system subject to certain
25 constraints (Jamian et al. 2014; Martins and Lambe 2013; Valdebenito and Schuëller 2010; Wu et al.
26 2021). An optimization problem can be formulated as:

$$\begin{aligned} & \text{Find } \mathbf{X}^* = \{X_1^*, X_2^*, \dots, X_n^*\} \\ & \text{to minimize } f(\mathbf{X}) \\ & \text{subject to } G_i(\mathbf{X}) \leq 0, (i = 1, 2, \dots, NC) \\ & \quad \mathbf{X}^l \leq \mathbf{X} \leq \mathbf{X}^u, \end{aligned} \tag{1}$$

28 where \mathbf{X} , n , f , G_i , NC , \mathbf{X}^l and \mathbf{X}^u are the design variable vector, number of design variables,
29 objective function, the i -th constraint function, number of constraints, lower bound vector of design
30 variables, and upper bound vector of design variables, respectively. Note that the design variables are
31 constrained in a range of upper and lower bounds, i.e., $\mathbf{X} \in \mathbf{X}^l = [\mathbf{X}^l, \mathbf{X}^u]$ where the superscript “ l ”
32 denotes that they are represented as an interval. The complexity of the design optimization problem is,
33 to some extent, determined by the number of design variables n and the size of the design space \mathbf{X}^l
34 (Jamian et al. 2014). In general, design variables are chosen as much as possible based on the
35 experience of designers and engineers in the initial design stage. This may result in a high-dimensional
36 complex optimization model (Jamian et al. 2014; Martins and Lambe 2013).

37 High-dimensional complex optimization problems often encounter obstacles that mainly come
38 from two aspects. First, the evaluation of the numerical model associated with a system often requires a
39 considerable computational cost that may take several hours for a single simulation, and the design
40 optimization usually requires hundreds or even thousands of iterative evaluations (Cho et al. 2014).
41 Therefore, the computational cost of high-dimensional optimization problems is usually expensive.
42 Second, optimization problems in engineering practice are often multidisciplinary, which will increase
43 the complexity of the problem and can lead to the failure of convergence to an optimal solution (Cho et
44 al. 2014; Spagnol et al. 2019; Wang et al. 2021, 2018). It is worth noting that engineers need to
45 repeatedly utilize the established optimization model many times during the product design iteration

process. Thus, high-dimensional complex optimization models are often unsuitable for subsequent use by engineers. In this situation, an effective approach, that is, design optimization based on pre-treatment of variables or so-called optimization with variable screening, is to perform design optimization in two stages (Spagnol et al. 2019; Wang et al. 2018). First, a sensitivity analysis is performed to rank the effect of all input variables and identify the most influential ones. Then, the optimization problem is remodeled by considering only these selected influential variables, while the other noninfluential variables are fixed at specific values in its space. It should be noted that variable screening is not the same as variable reformulation or feature projection, such as principal component analysis (Jolliffe 2002) or active subspace (Constantine et al. 2013) where the design space is changed.

Sensitivity analysis (also known as importance analysis) is a crucial step in many applications (Borgonovo and Plischke 2016; Wei et al. 2015). Through sensitivity analysis we gain essential insights into model behaviour, their structure and their response to changes on the model inputs (Borgonovo and Plischke 2016). In the past few decades, several sensitivity analysis methods have been developed, such as difference-based methods (Sobol' and Kucherenko 2009), parametric regression techniques (Härdle and Simar 2003), random forest techniques (Breiman 2001), variance-based methods (Homma and Saltelli 1996; Sobol' 1993) and moment-independent methods (Borgonovo 2007). Among them, variance-based methods have been particularly popular since the works of Sobol' (Sobol' 1993; Sobol' and Kucherenko 2009) were published (Homma and Saltelli 1996), and have been effectively applied to many engineering problems (Zhang et al. 2020).

Sensitivity analysis has emerged as a variable screening tool for high-dimensional complex optimization problems in various disciplines (Cho et al. 2014; Fesanghary et al. 2009; Li et al. 2020; Liu et al. 2020; Lu et al. 2015; Spagnol et al. 2019). In statistics, important variables among all candidate variables were accurately identified by a data-based sensitivity analysis (Duarte Silva 2001). Especially in statistical learning theory, different kinds of sensitivity analysis methods have been used to choose a subset of all input variables to model the system effectively (Guyon and Elisseeff 2003; Marra and Wood 2011; Marrel et al. 2008). In hydrology and earth systems (Li et al. 2013b),

72 qualitative sensitivity analysis methods were employed to find 2-8 important variables from a total of
73 40 variables, and the total effect of Sobol's sensitivity method was used to quantify the contribution of
74 each variable to the total variance of the model output (Li et al. 2013b). In addition, sensitivity analysis
75 was used as a screening tool to reduce the computational cost associated with multi-objective design
76 and rehabilitation of water distribution systems (Fu et al. 2012). In power and energy systems,
77 sensitivity analysis was adopted to quantitatively compare the impacts of 24 variables in three major
78 performances of a net-zero energy building (a promising solution to the worsening energy and
79 environmental problems) (Zhang et al. 2020). Also, sensitivity analysis-based multi-objective
80 optimization was performed to select the important operating parameters of a sinter cooler, thus
81 achieving the optimal indicator parameters and obtaining the corresponding operating conditions (Tian
82 et al. 2018). In the domain of structural design, sensitivity analysis methods were introduced or
83 modified to carry out the design optimization of aeronautical hydraulic pipelines, which demonstrated
84 that sensitivity-based variable screening methods can to some extent improve the efficiency of the
85 optimization (Li et al. 2020; Wang et al. 2018; Zhang et al. 2019). Moreover, sensitivity-based variable
86 screening methods have been used for automotive crashworthiness design (Craig et al. 2005),
87 composite fuselage frame design (Gao et al. 2019), occupant restraint system design (Liu et al. 2020),
88 thin-walled structure design, and dynamic design optimization of multi-motor driving transmission
89 systems (Shu et al. 2018).

90 Regarding the sensitivity indices that the above-mentioned works used, most of them are
91 variance-based measures, such as Sobol' indices. However, for the variable screening of optimization
92 problems, variance-based indices may have some limitations because they only focus on the effect of a
93 variable or multiple variables on the total variance of the model output rather than the model output
94 itself, which may fail to provide a reasonable evaluation of the importance of each input (Fort et al.
95 2016; Spagnol et al. 2019). Moreover, variance-based indices are appropriately implemented in a
96 probabilistic framework where inputs are represented by probabilistic information (e.g., a normal
97 distribution or uniform distribution). However, the design variables of an optimization problem are

98 usually described by interval models where no probabilistic information can be used (Martins and
99 Lambe 2013). A compromise treatment is to directly consider the interval design variables as normal
100 distribution or uniform distribution (Arwade et al. 2010; Fesanghary et al. 2009; Zhang et al. 2020),
101 which is a clear violation of the interval paradigms as artificial information is added to the analysis
102 (Chang et al. 2021; Zhou et al. 2021). There are relatively few works related to sensitivity analysis of
103 interval variables (Faes and Moens 2020; Wang et al. 2018). The available approach seems to be the
104 work of Wang et al. (Wang et al. 2018), which is also used as screening tools in the design optimization
105 problem. Unfortunately, Wang's approach struggles with some drawbacks: the considered output has
106 no clear physical meaning, and the indices may become inadequate in specific circumstances, which
107 will be elaborated and compared in this work. Recently, Chang et al. (Chang et al. 2022) proposed a
108 new interval sensitivity index, denoted as interval-based sensitivity index in the following, which can
109 provide an intuitive interpretation on the behaviour of model response with respect to interval inputs.
110 The model response can be regarded as the objective function of a design optimization problem, and
111 the interval inputs are exactly consistent with the interval constraints of design variables. In this work,
112 the interval-based sensitivity index is employed to screen the influential design variables for
113 high-dimensional complex optimization problems. Meanwhile, the effectiveness of the interval-based
114 sensitivity index will be compared with the indices of Sobol' and Wang, by its ability to find the
115 influential variables.

116 The remainder of this work is organized as follows. Firstly, the interval-based sensitivity index is
117 reviewed and is compared with other indices by a test function. In accordance with the design
118 optimization strategy based on the variable screening by sensitivity analysis, which is explained by two
119 illustrative optimization examples. Subsequently, the design optimization strategy is applied to an
120 aeronautical hydraulic pipeline system. Finally, the conclusions are drawn.

122 **Review and interpretation of the interval-based sensitivity index**

123 In this section, the general concept of the interval field and its normalized form are introduced to

124 discuss the connection between the interval field and variable sensitivity. Then, the interval-based
 125 sensitivity index, with a corresponding computational strategy, is reviewed, and its related
 126 characteristics and advantages are explained with the help of a test function. The index will be used to
 127 rank all input variables and screen the influential variables in next sections.

128

129 **Interval field**

130 A model $Y = f(\mathbf{X})$, with all classes of functions $f: \mathbb{R}^n \mapsto \mathbb{R}, \mathbf{X} \rightarrow Y$, is considered, where
 131 $\mathbf{X} = (X_1, X_2, \dots, X_n)$ is the vector of n -dimensional input variables and Y is the output. As reported
 132 in some optimization studies (Faes et al. 2017; Jiang et al. 2014; Wang et al. 2019, 2021), the design
 133 variables \mathbf{X} are assumed to be independent and expressed by the interval model as

134
$$X_i \in X'_i = [X_i^l, X_i^u], \quad (2)$$

135 where the superscript “ I ” denotes that the parameter is interval valued, $i = 1, 2, \dots, n$, X'_i and X_i^u
 136 with $X_i^l \leq X_i^u$ being respectively the lower and upper bounds of X_i . In addition, an interval can be
 137 represented by its centre value $X_i^c = (X_i^u + X_i^l)/2$ and its radius $X_i^r = (X_i^u - X_i^l)/2$. In case \mathbf{X}
 138 belongs to an interval vector \mathbf{X}^I , the output is also an interval, which is defined as

139
$$Y^I = [Y^l, Y^u] = [f^l, f^u] = [\min_{\mathbf{X} \in \mathbf{X}^I} f(\mathbf{X}), \max_{\mathbf{X} \in \mathbf{X}^I} f(\mathbf{X})]. \quad (3)$$

140 When X_i is fixed to a specific value in the interval $[X_i^l, X_i^u]$ and all other inputs are intervals,
 141 the corresponding output $Y_{X_i}^I$ is a subinterval of Y^I , i.e., $Y_{X_i}^I \subseteq Y^I$. The bounds of $Y_{X_i}^I$ are
 142 calculated as

143
$$\begin{aligned} Y_{X_i}^I &= [Y_{X_i}^l, Y_{X_i}^u] = [f^l(X_i), f^u(X_i)] \\ &= [\min_{\mathbf{X}_{-i} \in \mathbf{X}_{-i}^I} f(X_1, \dots, X_{i-1}, X_i, X_{i+1}, \dots, X_n), \max_{\mathbf{X}_{-i} \in \mathbf{X}_{-i}^I} f(X_1, \dots, X_{i-1}, X_i, X_{i+1}, \dots, X_n)], \end{aligned} \quad (4)$$

144 where \mathbf{X}_{-i} denotes the vector of all input variables except X_i and \mathbf{X}_{-i}^I denotes the interval vector
 145 associated with all variables except for X_i^I . Furthermore, when X_i loops through every element
 146 within $[X_i^l, X_i^u]$, the output will be an interval field $f^I(X_i)$, which is shown in Fig. 1 (A). The
 147 whole interval field $f^I(X_i)$ is enveloped by the lower bound $f^l(X_i)$ and upper bound $f^u(X_i)$,
 148 with $f^l(X_i) \leq f^u(X_i)$. The centre value and radius of the interval field can be defined as (Jiang et al.

149 2014)

150
$$f^c(X_i) = \frac{f^u(X_i) + f^l(X_i)}{2} \quad (5)$$

151 and

152
$$f^r(X_i) = \frac{f^u(X_i) - f^l(X_i)}{2}. \quad (6)$$

153 According to interval theory, the centre value $g^c(X_i)$ reflects the general degree of the interval field,
154 and the radius reflects the deviation degree of the interval field.

155 To facilitate the comparison of interval quantities and have a clearer and more intuitive
156 interpretation of the relationships between interval variables and the model output, the interval field can
157 be normalized as (Jiang et al. 2014)

158
$$f^l(X_i) = f^l(X_i^c + X_i^r \delta_i) = g^l(\delta_i), \quad (7)$$

159 where $\delta_i \in [-1, 1]$ is the normalized interval variable. Accordingly, the interval field $f^l(X_i)$ is
160 transformed into the normalized interval field $g^l(\delta_i)$ (shown in Fig. 1 (B)) which can be described by
161 $g^c(\delta_i)$ and $g^r(\delta_i)$:

162
$$g^c(\delta_i) = \frac{g^u(\delta_i) + g^l(\delta_i)}{2} \quad (8)$$

163
$$g^r(\delta_i) = \frac{g^u(\delta_i) - g^l(\delta_i)}{2}. \quad (9)$$

164

165 ***A recently proposed interval-based sensitivity index***

166 For all of the input variables X_1, X_2, \dots, X_n , the corresponding normalized interval field $g^l(\delta_i)$
167 ($i = 1, 2, \dots, n$) is usually different, and the difference between them is mainly determined by the
168 influences of model inputs \mathbf{X} on the model output Y (Chang et al. 2022). This is reflected in the
169 radius of the interval field $g^l(\delta_i)$. Two special examples are shown in Fig. 1 (C) and (D):

170 (i) In Fig. 1 (C), the lower bound $g^l(\delta_i)$ is always equal to Y^l (i.e., $g^l(\delta_i) \equiv Y^l$) and the upper
171 bound $g^u(\delta_i)$ is always equal to Y^u (i.e., $g^u(\delta_i) \equiv Y^u$), which indicates that no matter what
172 value X_i takes in the interval $[X_i^l, X_i^u]$, the model output $Y_{X_i}^l$ remains unchanged and equals
173 Y^l (i.e., $Y_{X_i}^l \equiv Y^l$). In this case, the input variable X_i has no influence on the model output,

174 making X_i a noninfluential variable.

175 (ii) In Fig. 1 (D), the lower bound $g'(\delta_i)$ and the upper bound $g''(\delta_i)$ coincide with each other, i.e.,
176 $g'(\delta_i) \equiv g''(\delta_i)$, which indicates that the uncertainty of the model output Y is eliminated when
177 X_i takes a specific value in the interval $[X'_i, X''_i]$. In this case, the model output is dominated
178 by the input variable X_i , which makes X_i an important variable.

179 For the most common situation of the normalized interval field $g'(\delta_i)$ shown in Fig. 1 (E), the
180 whole area (surrounded by four lines $Y = Y'$, $Y = Y''$, $\delta_i = -1$ and $\delta_i = 1$) is divided into three
181 parts: A_u enclosed by $g''(\delta_i)$ and $Y = Y''$, A_l enclosed by $g'(\delta_i)$ and $Y = Y'$, and A_{field}
182 enclosed by $g'(\delta_i)$ and $g''(\delta_i)$. According to the description, the larger A_{field} is, the less important
183 the variable is (e.g., the case of Fig. 1 (C)). In contrast, the smaller A_{field} is, the more important the
184 variable is (e.g., the case of Fig. 1 (D)). Therefore, an interval sensitivity index C_i was defined by
185 Chang et al. (Chang et al. 2022) as

$$186 C_i = \frac{A_u(i) + A_l(i)}{A_{total}(i)}, \quad (10)$$

187 where $A_{total}(i) = A_u(i) + A_l(i) + A_{field}(i)$. Furthermore, C_i can be derived by the following
188 expression (Chang et al. 2022):

$$189 C_i = \frac{A_u(i) + A_l(i)}{A_{total}(i)} \\ = \frac{A_{total}(i) - A_{field}(i)}{A_{total}(i)} = 1 - \frac{A_{field}(i)}{A_{total}(i)} \\ = 1 - \frac{1}{2(Y'' - Y')} \int_{-1}^1 (g''(\delta_i) - g'(\delta_i)) d\delta_i. \quad (11)$$

190 In addition, the interval sensitivity index can be extended when we wish to know the joint
191 contribution of two or more variables for the model output, which are derived in Appendix A. More
192 information about the interval sensitivity index can be found in (Chang et al. 2022).

193 After introducing the interval sensitivity index, a test function will be studied next to compare the
194 sensitivity analysis results of three types of indices including the interval-based sensitivity index,
195 Sobol' indices (reviewed in Appendix B), and Wang's indices (reviewed in Appendix C).

197 **An illustrative function to interpret the interval sensitivity index**

198 A four-variable function is considered as (Chang et al. 2021)

199
$$f(\mathbf{X}) = X_1 X_2 - 2X_2 X_3 + 3X_3 X_4 - 4X_4 X_1 + 4X_1 X_2 X_3 X_4, \quad (12)$$

200 where $\mathbf{X} = (X_1, X_2, X_3, X_4)$ are the input variables. Two cases are considered for this function, which
201 are listed in Table 1. It should be noted that the Sobol' indices in the following are calculated on the
202 premise that all input variables are assumed to be uniformly distributed in its interval. Sobol's indices
203 are included for comparative reasons, and stem from the case where an analyst would invoke the
204 maximum entropy principle to first estimate a distribution based on the available information (i.e.,
205 bounds), followed by the sensitivity analysis. Further, it should be noted that both sets of indices have a
206 fundamentally different meaning behind them. Nonetheless, in view of selecting the most appropriate
207 parameters to perform optimization, the usage of these indices is similar, which warrants comparison.

208 For Case 1, the results of C_i are shown in Fig. 2 (A), and its corresponding normalized interval
209 fields are shown in Fig. 2 (D), where the order of dashed area is $A_3 > A_2 \approx A_4 > A_1$. This indicates that
210 the order of the variable importance is $X_3 > X_2 \approx X_4 > X_1$. In addition, the results of Wang's indices
211 (ζ_i and ς_i) and Sobol' indices (S_i and S_{Ti}) are shown in Fig. 2 (B) and (C), respectively. The
212 variable importance results of the three types of indices are the same (i.e., $X_3 > X_2 \approx X_4 > X_1$)
213 except that the result of radius sensitivity ς_i is $X_3 > X_2 \approx X_4 \approx X_1$.

214 For Case 2, the results of C_i are shown in Fig. 3 (A), and its corresponding normalized interval
215 fields are shown in Fig. 3 (D), where the order of dashed area is $A_4 > A_1 \approx A_3 > A_2$. According to Fig.
216 3 (A) and (D), $C_4 > C_1 \approx C_3 > C_2$ indicates that the order of the variable importance is
217 $X_4 > X_1 \approx X_3 > X_2$. In Fig. 3 (B), the orders of Wang's indices are $\zeta_1 > \zeta_2 > \zeta_4 > \zeta_3$ and
218 $\varsigma_1 > \varsigma_3 > \varsigma_4 > \varsigma_2$, respectively. In Fig. 3 (C), the order of Sobol' indices $S_i \approx 0$ ($i = 1, 2, 3, 4$) and
219 $S_{T4} > S_{T1} > S_{T3} > S_{T2}$, respectively. The variable importance result of the total effect index S_{Ti} is
220 almost the same as the interval-based sensitivity index C_i . Nevertheless, the variable importance order
221 cannot be obtained by Wang's indices because the ζ_i and ς_i results are inconsistent.

223 ***Discussion on the interval sensitivity index***

224 According to the introduction of the interval-based sensitivity index and the analysis results of the
225 illustrative function, four aspects of discussions need to be emphasized to offer deeper insights into the
226 index.

227 **First**, three characteristics of the interval-based sensitivity index need to be emphasized:

228 (i) As shown in previous sections, the proposed index C_i is the ratio of the left dashed to the total
229 rectangular area; therefore, the lower bound of C_i is 0, while the upper bound of C_i is 1, i.e.,
230 $0 \leq C_i \leq 1$. The larger C_i is, the more important X_i is. Conversely, the smaller C_i is, the less
231 important X_i is.

232 (ii) If $C_i = 0$ (as shown in Fig. 1 (C)), the uncertainty of X_i has no influence on the model output
233 Y . Therefore, X_i is a noninfluential variable in this case.

234 (iii) If $C_i = 1$ (as shown in Fig. 1 (D)), the uncertainty of X_i has dominant influence on the model
235 output Y . Thus, X_i is the most important variable in this case.

236 **Second**, similar to conventional sensitivity indices, such as Sobol' indices (Sobol' 1993; Sobol'
237 and Kucherenko 2009; Wei et al. 2015a) and Wang's indices (Wang et al. 2018), the interval-based
238 sensitivity index C_i can be used for the sensitivity analysis of the input variables, thus providing a
239 deeper understanding of the considered system and more comprehensive analysis results for
240 engineering designers. At the same time, the index can be used as a variable screening tool for
241 optimization problems, which will be specifically implemented in next sections. In particular, those
242 variables with relatively large index C_i are selected as influential variables, and then the optimization
243 problem is solved by considering only these selected influential variables, while the other
244 noninfluential variables are evaluated at specific values in its space. Moreover, as shown in Fig. 2 (D)
245 and Fig. 3 (D), the interval-based sensitivity analysis can not only rank the importance of input
246 variables, but also present the behaviour of model response with respect to each interval input, thus
247 providing the guidance for the determination/realization of value-fixation of noninfluential variables.
248 That is to say, fixing these noninfluential variables can be determined with the help of the

249 interval-based sensitivity analysis results, rather than crudely fix all noninfluential variables at its initial
250 values (e.g., lower bounds, upper bounds, or centre values). The specific implementation will be
251 elaborated in next section.

252 **Third**, the classical Sobol' indices (reviewed in Appendix B) are variance-based indices (Sobol'
253 1993; Sobol' and Kucherenko 2009; Wei et al. 2015). For the design optimization with variable
254 screening, selecting Sobol' indices as a screening tool may have three limitations, which are analyzed
255 as follows:

256 (i) Sobol' indices reflect the contribution of input variables to the model output variance (rather than
257 the model output itself), which is just a variance-based criterion, rather than a comprehensive
258 characteristic description of the model output (Cho et al. 2014).

259 (ii) In design optimization problems, the design variables are often confined by the lower and upper
260 bounds of intervals rather than characterized by probabilistic models. It may be inappropriate to
261 directly consider the design variable as a specific probabilistic model (e.g., normal distribution or
262 uniform distribution).

263 (iii) Sobol' indices can only offer the importance ranking results, but not the behaviour of model
264 response with respect to each interval input. Hence, Sobol' indices may not provide sufficient
265 information for fixing the value of noninfluential variables.

266 **Fourth**, Wang's indices (Wang et al. 2018) (reviewed in Appendix C) can be used to identify
267 influential variables in design optimization problems, though three drawbacks need to be emphasized:

268 (i) Wang's indices reflect the contribution of input variables to $\eta = Y^c/Y^r$, which is the ratio of the
269 centre value to the radius of the model output, rather than the model output itself. Moreover, η
270 has no clear physical meaning.

271 (ii) According to the introduction of Appendix C, $\eta = Y^c/Y^r$ is equal to 0 when $Y^c = 0$. In this
272 case, the definition of Eqs. (C6) and (C7) (i.e., $\zeta_i = |\eta - [\eta|X_i]^c|/\eta$ and $\varsigma_i = [\eta|X_i]^r/\eta$) are
273 invalid because η is the denominator in Eqs. (C6) and (C7). Therefore, Wang's indices can only
274 be used in the case of $Y^c \neq 0$. Meanwhile, when η is approximately equal to 0 (i.e., $\eta \approx 0$), the

275 results of ζ_i and ς_i are likely to be influenced by calculation errors, which can be clearly
276 realized by the comparation results of Case 1 and Case 2 in the illustrative function of the
277 previous section.

278 (iii) Same as Sobol' indices, Wang's indices cannot offer insight on the behaviour of model response
279 with respect to each interval input. As a result, Wang's indices may not be informative for fixing
280 values of noninfluential variables. The details will be elaborated and examined in next sections.

281 In addition, the effectiveness and superiorities of the interval-based sensitivity index will be
282 further compared with Sobol' indices and Wang's indices by its ability to find the influential variables
283 of design optimization problems in the illustration examples of next section.

284

285 ***Computational strategy for calculating the interval sensitivity index***

286 As shown in Eq. (11), the interval-based sensitivity index C_i can be calculated using Y^l , Y^u ,
287 $g^l(\delta_i)$, and $g^u(\delta_i)$. The calculation of them is addressed in detail in the following.

288

289 ***Calculation of Y^l and Y^u***

290 The calculation of Y^l and Y^u is a classical interval analysis problem, which has been discussed
291 in depth by Faes et al. (Faes et al. 2017; Faes and Moens 2020). In this section, Y^l and Y^u are
292 obtained by solving the following two optimisation problems:

$$\begin{aligned} & \text{Find } \boldsymbol{\delta}^* = \{\delta_1^*, \delta_2^*, \dots, \delta_n^*\} \\ & \text{to minimize } g(\boldsymbol{\delta}) \\ & \text{subject to } -1 \leq \delta_i \leq 1, (i = 1, 2, \dots, n) \end{aligned} \quad (13)$$

294 and

$$\begin{aligned} & \text{Find } \boldsymbol{\delta}^{**} = \{\delta_1^{**}, \delta_2^{**}, \dots, \delta_n^{**}\} \\ & \text{to maximize } g(\boldsymbol{\delta}) \\ & \text{subject to } -1 \leq \delta_i \leq 1, (i = 1, 2, \dots, n). \end{aligned} \quad (14)$$

296 We can observe that $Y^l = g(\boldsymbol{\delta}^*)$ and $Y^u = g(\boldsymbol{\delta}^{**})$. In this work, the surrogate optimisation (SO)
297 algorithm (Wang and Shoemaker 2014), integrated as “surrogateopt” function in MATLAB software, is
298 adopted to implement the two optimisation problems (i.e., Eqs. (13) and (14)) to obtain Y^l and Y^u .

299

300 *Calculation of $g^l(\delta_i)$ and $g^u(\delta_i)$*

301 For the calculation of $g^l(\delta_i)$ and $g^u(\delta_i)$, a double-loop strategy can be adopted (Chang et al.
 302 2022). In the inner layer, the minimum and maximum values $g^l(\delta_i)$ and $g^u(\delta_i)$ of the output
 303 response for the given value δ_i are obtained by solving the following two optimization problems:

304

$$\begin{aligned} \text{Find } \boldsymbol{\delta}'_{-i} &= \{\delta'_1, \delta'_2, \dots, \delta'_{i-1}, \delta'_{i+1}, \dots, \delta'_n\} \\ \text{to minimize } g(\boldsymbol{\delta}) \\ \text{subject to } -1 \leq \boldsymbol{\delta}_{-i} &\leq 1 \\ \delta_i &= \delta_{i(h)} \end{aligned} \quad (15)$$

305 and

306

$$\begin{aligned} \text{Find } \boldsymbol{\delta}''_{-i} &= \{\delta''_1, \delta''_2, \dots, \delta''_{i-1}, \delta''_{i+1}, \dots, \delta''_n\} \\ \text{to maximize } g(\boldsymbol{\delta}) \\ \text{subject to } -1 \leq \boldsymbol{\delta}_{-i} &\leq 1 \\ \delta_i &= \delta_{i(h)}, \end{aligned} \quad (16)$$

307 where $h = 1, 2, \dots, n_{\text{sample}}$, n_{sample} denotes the number of generated grid points of δ_i . We can observe
 308 that $g^l(\delta_{i(h)}) = g(\boldsymbol{\delta}'_{-i}, \delta_{i(h)})$ and $g^u(\delta_{i(h)}) = g_h(\boldsymbol{\delta}''_{-i}, \delta_{i(h)})$. Also, SO algorithm as described in previous
 309 section is adopted to solve Eqs. (15) and (16). In the outer layer of the double-loop strategy, the lower
 310 bound curve $g^l(\delta_i)$ and upper bound curve $g^u(\delta_i)$ of the interval field $g^l(\delta_i)$ can be
 311 approximately fitted by global metamodeling with adaptive sampling. The details of global
 312 metamodeling method are described in (Chang et al. 2022) and the practical implementation of the
 313 strategy is summarized in Algorithm 1.

314 The optimisation algorithm SO is called to calculate the lower/upper bounds $g^l(\delta_{i(h)})/g^u(\delta_{i(h)})$ at
 315 a series of grid points $\delta_{i(h)}$. The initial points $\{\delta_{i(1)}, \dots, \delta_{i(n_m)}\}$ and their corresponding lower/upper
 316 bounds $\{g^l(\delta_{i(1)}), \dots, g^l(\delta_{i(n_m)})\}/\{g^u(\delta_{i(1)}), \dots, g^u(\delta_{i(n_m)})\}$ are firstly used to construct a metamodel,
 317 then the new point $\delta_{i(\text{new})}$ is selected, by maximizing the mean square error (Liu et al. 2018), to update
 318 the model until the stopping criterion is met. Finally, $g^l(\delta_i)$ and $g^u(\delta_i)$ are obtained to calculate the
 319 interval-based sensitivity index C_i .

320

321 **Design optimization with variable screening by the interval-based sensitivity**

322 **index**

323 ***General process***

324 For the design optimization model expressed in Eq. (1), all input variables $\mathbf{X} = \{X_1, X_2, \dots, X_n\}$
325 can be divided into two categories, i.e., top influential variables $\mathbf{X}_{\text{Top}} = \{X_{\text{Top}(1)}, X_{\text{Top}(2)}, \dots, X_{\text{Top}(m)}\}$
326 and noninfluential variables $\mathbf{X}_{\sim\text{Top}} = \{X_{\sim\text{Top}(1)}, X_{\sim\text{Top}(2)}, \dots, X_{\sim\text{Top}(n-m)}\}$, by sensitivity ranking results.
327 The subscript “Top” refers to variables that are significantly more influential than other variables. As
328 can be seen, $\mathbf{X} = \{\mathbf{X}_{\text{Top}}, \mathbf{X}_{\sim\text{Top}}\}$ and $m \leq n$. Then, the design optimization problem can be
329 reformulated as

$$\begin{aligned} & \text{Find } \mathbf{X}_{\text{Top}}^* = \{X_{\text{Top}(1)}^*, X_{\text{Top}(2)}^*, \dots, X_{\text{Top}(m)}^*\} \\ & \text{to minimize } f(\mathbf{X}_{\text{Top}}, \mathbf{X}_{\sim\text{Top}}) \\ & \text{subject to } G_i(\mathbf{X}_{\text{Top}}, \mathbf{X}_{\sim\text{Top}}) \leq 0, (i = 1, 2, \dots, NC) \\ & \quad \mathbf{X}_{\text{Top}}^l \leq \mathbf{X}_{\text{Top}} \leq \mathbf{X}_{\text{Top}}^u \\ & \quad \mathbf{X}_{\sim\text{Top}} = \mathbf{X}_{\sim\text{Top}}^{\text{sv}}, \end{aligned} \tag{17}$$

330 where $\mathbf{X}_{\text{Top}}^l$ and $\mathbf{X}_{\text{Top}}^u$ are the lower and upper bound vectors of influential design variables \mathbf{X}_{Top} ,
331 respectively. $\mathbf{X}_{\sim\text{Top}}^{\text{sv}}$ is the selected specific value vector of the noninfluential variables $\mathbf{X}_{\sim\text{Top}}$. As
332 illustrated in the discussion on the interval sensitivity index, Sobol’ and Wang’s indices cannot offer
333 insight on the behaviour of model response with respect to each interval input. Therefore, all
334 noninfluential variables $\mathbf{X}_{\sim\text{Top}}$ are crudely fixed at its centre values (i.e., $\mathbf{X}_{\sim\text{Top}} = \mathbf{X}_{\sim\text{Top}}^c$) (or lower
335 bounds (i.e., $\mathbf{X}_{\sim\text{Top}} = \mathbf{X}_{\sim\text{Top}}^l$) and upper bounds (i.e., $\mathbf{X}_{\sim\text{Top}} = \mathbf{X}_{\sim\text{Top}}^u$)). Meanwhile, for the
336 interval-based sensitivity index, the k -th noninfluential variable $X_{\sim\text{Top}(k)}$ ($k = 1, 2, \dots, n-m$) is fixed
337 as a specific value $X_{\sim\text{Top}(k)}^{\text{sv}}$, where $X_{\sim\text{Top}(k)}^{\text{sv}} \in [X_{\sim\text{Top}(k)}^l, X_{\sim\text{Top}(k)}^u]$ is the value that corresponds to the
338 minimum of the whole interval field $f'(X_{\sim\text{Top}(k)})$, i.e., $f'(X_{\sim\text{Top}(k)}^{\text{sv}}) = Y^l$. Correspondingly, when
339 solving a maximization problem, the specific value $X_{\sim\text{Top}(k)}^{\text{sv}}$ will be the value that corresponds to the
340 maximum of the whole interval field $f'(X_{\sim\text{Top}(k)})$, i.e., $f'(X_{\sim\text{Top}(k)}^{\text{sv}}) = Y^u$. The general process of the
341 design optimization with variable screening can be summarized in Fig. 4.
342

343 It can be seen that the objective function f and constraint function G_i change from the original
344 n -dimensional functions to m -dimensional functions, and the number of the design variables is reduced

345 from the original n to m , which will effectively simplify the optimization problem. It should be noted
346 that the specific value of m is determined by the designers based on sensitivity analysis results, model
347 accuracy requirements and acceptable calculating costs, which will be specifically demonstrated by
348 optimization examples in the next section. In addition, for a complex optimization problem in
349 engineering practice (e.g., the aeronautical hydraulic pipeline) where the model response is obtained by
350 a time-consuming black box (e.g., finite element analysis), the sensitivity analysis may require a lot of
351 computational cost that designers cannot afford. In this case, metamodels can be adopted to reduce
352 intensive computational costs of the sensitivity analysis (Chang et al. 2022).

353

354 ***Illustrative examples of the design optimization with variable screening***

355 Two illustrative optimization examples are conducted to examine the design optimization strategy
356 and to compare the ability of different sensitivity indices to find the optimal results (including the
357 maximum result and the minimum result) and their effect on variable screening. It should be noted that
358 the Sobol' indices are calculated on the premise that all input variables are assumed to be uniformly
359 distributed in its interval. Besides, the sequential quadratic programming (SQP) optimizer is employed
360 for the two illustrative optimization examples.

361

362 ***A ten-dimensional optimization example***

363 A ten-dimensional optimization example (Wang et al. 2018) is expressed as

$$\begin{aligned} \text{Find } \mathbf{X}^* &= \{X_1^*, X_2^*, \dots, X_{10}^*\} \\ \text{to maximize/minimize } f(\mathbf{X}) &= X_1^2 + X_2^2 - X_3^2 - X_{10}^2 + X_1 X_2 - 14X_1 - 16X_2 \\ &\quad + (X_3 - 10)^2 + 4(X_4 - 5)^2 + (X_5 - 3)^2 + 2(X_6 - 1)^2 + 5X_7^2 \quad (18) \\ &\quad + 7(X_8 - 11)^2 + 2(X_9 - 10)^2 + (X_{10} - 7)^2 + 20X_3 + 14X_{10} - 50 \\ \text{subject to } X_i^l &\leq X_i \leq X_i^u, \quad (i = 1, 2, \dots, 10), \end{aligned}$$

365 where the lower and upper bounds of all interval variables are assumed to be 5 and 6, respectively, i.e.,
366 $X_i^l = 5$ and $X_i^u = 6$ for $i = 1, 2, \dots, 10$. The actual lower and upper bounds of the model output are
367 $f'(\mathbf{X}) = 391.75$ and $f''(\mathbf{X}) = 572$, and the corresponding centre and radius are

368 $f^c(\mathbf{X}) = 481.875$ and $f^r(\mathbf{X}) = 90.125$.

369 As shown in Fig. 5 (A), the importance ranking obtained by the interval-based sensitivity index
370 C_i is $X_8 > X_7 > X_9 \approx X_6 > X_5 \approx X_4 > X_1 \approx X_2 > X_3 \approx X_{10}$. Fig. 5 (D) shows the normalized
371 interval field used to obtain C_i ($i = 1, 2, \dots, 10$). Fig. 5 (E) is the normalized interval field used to
372 obtain C_{78} , which indicates the joint contribution of X_7 and X_8 to the model output $f(\mathbf{X})$. The
373 importance ranking obtained by Wang's indices (Fig. 5 (B)) and Sobol' indices (Fig. 5 (C)) are the
374 same as that of the index C_i . It should be noted that the three types of sensitivity indices associated
375 with X_3 and X_{10} are equal to zero, (i.e., $C_3 = \zeta_3 = \varsigma_3 = S_3 = S_{T3} = 0$ and
376 $C_{10} = \zeta_{10} = \varsigma_{10} = S_{10} = S_{T10} = 0$), and the three types of indices associated with X_1 and X_2 are very
377 small and close to zero. The value of the model output is basically unchanged when these four variables
378 (X_3 , X_{10} , X_1 and X_2) change within its interval range. In contrast, the three types of indices
379 associated with X_8 , X_7 , X_6 and X_9 are obviously larger than other variables, which means that
380 X_8 , X_7 , X_6 and X_9 have a considerable influence on the model output.

381 In Fig. 5 (F), the optimization results (including the maximum value f_{\max} and minimum value
382 f_{\min}) as well as the computational cost (measured by N_{call} , i.e., the number of function calls for SQP
383 optimizer during the optimization process) corresponding to different sets of design variables are given.
384 In the horizontal abscissa, Top m ($m = 1, 2, \dots, 10$) represents the first m most influential design
385 variables according to the sensitivity analysis. For example, Top 4 means that X_8 , X_7 , X_6 and X_9
386 are considered in the optimization, and the rest are fixed at a specific value (such as centre values, i.e.,
387 $\mathbf{X}_{\sim\text{Top}} = \mathbf{X}_{\sim\text{Top}}^c$, or a set of selected values, i.e., $\mathbf{X}_{\sim\text{Top}} = \mathbf{X}_{\sim\text{Top}}^{sv}$) in its intervals. When all the
388 noninfluential variables are fixed at their centre values (i.e., $\mathbf{X}_{\sim\text{Top}} = \mathbf{X}_{\sim\text{Top}}^c$), the maximum and
389 minimum values are 544.99 and 413.00 in the case of Top 2, 564.00 and 396.00 in case of Top 4,
390 569.75 and 393.75 in the case of Top 6, and 572.00 and 391.75 in the case of Top 10 (all variables).
391 Meanwhile, when all the noninfluential variables are fixed at a set of selected values $\mathbf{X}_{\sim\text{Top}}^{sv}$ based on
392 the information of the interval-based sensitivity analysis result, the maximum and minimum values are
393 572.00 and 391.75 for all the case of Top m . Take the minimum optimization of Top 2 case as an

394 example, the Top 2 influential variables (i.e., X_8 and X_7) are selected as design variables while the
 395 noninfluential variables (i.e., $X_1 \sim X_6$, X_9 and X_{10}) are fixed at $\mathbf{X}_{\sim \text{Top}}^{\text{sv}}$. According to Fig. 5 (D),
 396 $\mathbf{X}_{\sim \text{Top}}^{\text{sv}} = \{X_1^l, X_2^c, X_3^{\forall}, X_4^l, X_5^l, X_6^l, X_9^u, X_{10}^{\forall}\}$ where the superscript \forall of X_3 and X_{10} means
 397 any value in its intervals because the change of X_3 and X_{10} have no effect on the model output, and
 398 the superscripts c , l and u are the centre value, lower bound and upper bound, respectively. At the same
 399 time, when performing maximization of Top 2 case, the fixed values for the noninfluential variables
 400 can be selected as $\mathbf{X}_{\sim \text{Top}}^{\text{sv}} = \{X_1^u, X_2^c, X_3^{\forall}, X_4^u, X_5^u, X_6^u, X_9^l, X_{10}^{\forall}\}$ based on the normalized interval
 401 field $g'(\delta_i)$ in Fig. 5 (D).

402 In addition, the number of function calls during the optimization process (including N_{call} of f_{\max}
 403 and f_{\min}) increases with the increase of variables. Satisfactory optimization results can be obtained by
 404 considering the influential design variables, e.g., Top 4, and the computational cost can be reduced by
 405 more than half in the case of Top 4. At the same time, when the noninfluential variables $\mathbf{X}_{\sim \text{Top}}$ are
 406 fixed at $\mathbf{X}_{\sim \text{Top}}^{\text{sv}}$, the optimal results (i.e., $f_{\max} = 572.00$ and $f_{\min} = 391.75$) of Top 10 (all variables)
 407 optimization can also be obtained by Top m ($m < 10$) optimization case, which can be seen in Fig. 5
 408 (F). In other words, it is effective and practical to perform design optimization with these influential
 409 variables selected by the interval-based sensitivity index C_i . Moreover, the interval-based sensitivity
 410 analysis can provide the behaviour of model response with respect to each interval inputs, so as to give
 411 the guidance for the determination/realization of value-fixation of noninfluential variables. As can be
 412 seen in Fig. 5 (F), this strategy is obviously useful for finding the minimum/maximum value of the
 413 problem.

414

415 *A twenty-dimensional optimization example*

416 A twenty-dimensional optimization example (Craig et al. 2005; Welch et al. 1992) is expressed as

Find $\mathbf{X}^* = \{X_1^*, X_2^*, \dots, X_{20}^*\}$

to maximize/minimize $f(\mathbf{X}) = 5X_{12}/(1 + X_1) + 5(X_4 - X_{20})^2 + X_5 + 40X_{19}^3 - 5X_{19}$

$$\begin{aligned} & + 0.05X_2 + 0.08X_3 - 0.03X_6 + 0.03X_7 - 0.09X_9 - 0.01X_{10} \\ & - 0.07X_{11} + 0.25X_{13}^2 - 0.04X_{14} + 0.06X_{15} - 0.01X_{17} - 0.03X_{18} \end{aligned} \quad (19)$$

subject to $X_i^l \leq X_i \leq X_i^u$, ($i = 1, 2, \dots, 20$).

The lower and upper bounds of all interval variables are assumed to be -0.5 and 0.5, respectively,

i.e., $X_i^l = -0.5$ and $X_i^u = 0.5$ for $i = 1, 2, \dots, 20$. The actual lower and upper bounds of the model output are $f^l(\mathbf{X}) = -8.152$ and $f^u(\mathbf{X}) = 13.3125$ (Craig et al. 2005; Welch et al. 1992), and the corresponding centre and radius are $f^c(\mathbf{X}) = 2.5803$ and $f^r(\mathbf{X}) = 10.7323$. The function is evidently nonlinear, and that there are six influential variables ($X_1, X_4, X_5, X_{12}, X_{19}$ and X_{20}) as discussed in (Craig et al. 2005; Welch et al. 1992).

The results of three types of indices (i.e., the interval-based sensitivity index, Wang's indices and Sobol' indices) are compared in Fig. 6, where (A) is the interval-based sensitivity index C_i , (B) is Wang's indices including the centre value sensitivity ζ_i and radius sensitivity ς_i and (C) is the Sobol' indices including the main effect S_i and the total effect S_{Ti} . The six influential variables are successfully identified by C_i , ζ_i , ς_i and S_{Ti} . It can be observed that the main effect S_i corresponding to X_1 is approximately equal to 0, primarily due to the interaction influence between X_1 and the most influential variable X_{12} in the response function. In addition, the variable importance orders obtained by the five indices are different from each other, where the top influential variables are listed in Fig. 6 (A)-(C).

To compare the ability of these three types of indices to find the influential variables, the optimization results (including the maximum value f_{\max} and minimum value f_{\min}) as well as the computational cost (measured by N_{call} , i.e., the number of function calls for SQP optimizer during the optimization process) corresponding to different sets of design variables are given in Fig. 7. Similar to the previous section, in the horizontal abscissa, Top m ($m = 1, 2, \dots, 20$) represents the first m most influential design variables according to the sensitivity analysis. Therefore, the optimization results gradually tend to the optimal solution (i.e., $f_{\max} = 13.3125$ and $f_{\min} = -8.152$) with the increase of design variables. Additionally, the number of function calls (including N_{call} of f_{\max} and f_{\min})

441 increases with the increase of variables. For the case of Top 1, the maximum and minimum values
 442 associated with five indices (C_i , ζ_i , ς_i , S_i and S_{Ti}) are the same, i.e., $f_{\max} = 2.5$ and
 443 $f_{\min} = -2.5$. In the case of Top 2, the maximum and minimum values associated with four indices (C_i ,
 444 ζ_i , ς_i and S_i) are the same ($f_{\max} = 5$ and $f_{\min} = -5$), while those associated with S_{Ti} are
 445 $f_{\max} = 3.75$ and $f_{\min} = -2.5$, so the ability of S_{Ti} is inferior to other four indices (C_i , ζ_i , ς_i and
 446 S_i) in the case of Top 2. The situations in the Top 3-6 and the Top 20 can be concluded in the same
 447 manner, where ς_i , S_{Ti} and S_i are inferior to C_i and ζ_i in the case of Top 3, ς_i and S_i are
 448 inferior to C_i , ζ_i and S_{Ti} in the case of Top 5, and S_i is inferior to the other four indices (i.e., C_i ,
 449 ζ_i , ς_i and S_{Ti}) in the case of Top 6. The number of inferiors (i.e., the number of times that the Top m
 450 extrema associated with an index is inferior to the Top m extrema associated with one of other four
 451 indices) of the five indices are shown in the top left corner of Fig. 7, where the interval-based
 452 sensitivity index C_i and the centre value sensitivity ζ_i of Wang's indices are obviously superior to
 453 the other three indices in this example.

454 In addition, it can be seen that the minimum result (-7.5) of the Top 3 associated with C_i is very
 455 close to the minimum result (-8.152) of the Top 20, and the corresponding numbers of function calls of
 456 the Top 3 and Top 20 are 40 and 820, respectively, where more than 95% of computational cost is
 457 saved. At the same time, the maximum result (12.5) of the Top 5 associated with C_i is very close to
 458 the maximum result (13.3125) of the Top 20, and the corresponding number of function calls of the Top
 459 5 and the Top 20 are 55 and 451, respectively, where more than 87% of the computational cost is saved.

460 Moreover, the above-discussed Top m ($m = 1, 2, \dots, 6$) optimization is performed in the case of
 461 the noninfluential variables are fixed at its centre values (i.e., $\mathbf{X}_{\sim\text{Top}} = \mathbf{X}_{\sim\text{Top}}^c$). When all the
 462 noninfluential variables are fixed at a set of selected values $\mathbf{X}_{\sim\text{Top}}^{sv}$ based on the information of the
 463 interval-based sensitivity analysis result, the maximum and minimum values are 13.3125 and -8.152 for
 464 all the case of Top m . Take the minimum optimization of Top 4 case as an example, the Top 4
 465 influential variables (i.e., X_{12} , X_1 , X_{19} and X_{20}) are selected as design variables while the
 466 noninfluential variables (i.e., $X_2 \sim X_{11}$ and $X_{13} \sim X_{18}$) are fixed at

467 $\mathbf{X}_{\sim\text{Top}}^{\text{sv}} = \{X_2^l, X_3^l, X_4^v, X_5^l, X_6^u, X_7^l, X_8^v, X_9^u, X_{10}^u, X_{11}^u, X_{13}^c, X_{14}^u, X_{15}^l, X_{16}^v, X_{17}^u, X_{18}^u\}$ which are selected
468 based on the normalized interval field $g'(\delta_i)$ of the interval-based sensitivity analysis. As can be seen
469 from above discussion, performing the design optimization with these few influential variables
470 (selected by the index C_i), while the rest of noninfluential variables are fixed at the selected values
471 $\mathbf{X}_{\sim\text{Top}}^{\text{sv}}$, is effective and practical.

472

473 **Application for the design of an aeronautical hydraulic pipeline**

474 In this section, the interval-based sensitivity index C_i will be applied to a practical engineering
475 problem of aeronautical hydraulic pipelines, which was first presented in Wang's work (Wang et al.
476 2018) and studied in (Li et al. 2020; Zhang et al. 2019; ZHOU et al. 2019). First, we introduce the
477 problem of aeronautical hydraulic pipelines, then perform the optimization design with variable
478 screening based on the interval-based sensitivity analysis result, before finally discussing the findings.

479

480 *Introduction of the aeronautical hydraulic pipelines*

481 For most modern aircrafts, hydraulic pipelines are functional units that transmit hydraulic oil to
482 drive a series of mechanisms on board (Ouyang et al. 2012; Tang et al. 2011), such as flaps, landing
483 gears, and folding mechanisms. At the same time, hydraulic pipelines undertake complex working
484 conditions, such as external shock, vibration, or other dynamic loads. In particular, aeronautical
485 hydraulic pipelines are quite different from those in other engineering areas, which is mainly reflected
486 in three aspects (Zhou et al. 2019):

487 (i) Low stiffness. The stiffness of aeronautical hydraulic pipelines is relatively low due to space and
488 weight constraints.

489 (ii) Long pipelines and a considerable number of curves. Aeronautical hydraulic pipelines are
490 relatively long because of the long distances between actuators and pumps. Meanwhile, hydraulic
491 pipelines are curved frequently, because of the arrangement of structural parts and the confined
492 space on board. This may have impacts on the stability of the pipelines.

493 (iii) Complicated vibration environment. There are many vibration sources, such as engines, pumps
494 and aerodynamics that can cause excitations of hydraulic pipelines.

495 In engineering practice, the stress and displacement are two quantities of concern, and the failure
496 of aeronautical hydraulic pipeline is mainly due to fatigue load caused by vibration. To be specific, the
497 stress values of all nodes of the hydraulic pipeline change with the excitation. In this study, the
498 excitation of hydraulic pipelines is considered as stochastic due to random external vibration, the
499 complexity of structures, and variations in aircraft loads (Wang et al. 2018). For a specific node,
500 standard deviation of stress reflects the degree of stress change in the whole vibration cycle. The
501 greater the standard deviation of stress, the easier the fatigue failure will occur. Therefore, the
502 maximum standard deviation of stress is chosen as the objective of optimisation design. Meanwhile, the
503 maximum standard deviation of displacement is treated as a constraint in this work. In general, a series
504 of hoops (which are usually dozens or even hundreds) are used to fix hydraulic pipelines, thus
505 preventing instability caused by long spans and excitation, which can obviously lower the stress and
506 displacement in the vibration environment (Wang et al. 2018; Zhou et al. 2019). Therefore, the
507 constraint location plays an important role on the safety of hydraulic pipelines. So, the coordinates of
508 the hoop locations are selected as design variables.

509 As shown in Fig. 8 (A), the finite element model of an aeronautical hydraulic pipeline is built in
510 ANSYS 17.1, and its related parameters are listed in the lower part of Fig. 8 (A) (Zhou et al. 2019).
511 ρ_P , D , t , ρ_f , T , P , E and μ represent the material density, outer radius, thickness, fluid density,
512 ambient temperature, internal pressure (which is caused by the flow of oil in pipeline), elastic modulus
513 and Poisson's ratio, respectively. Twenty-eight design variables (coordinates of hoops) are selected
514 from 21 hoop locations in Fig. 8 (B), which are listed in Table 2. It should be reminded that more than
515 one coordinate is considered at some hoop locations including 45, 62, 69, 72, 75 and 85. The stochastic
516 excitation is given in the form of an acceleration power spectral density (PSD) function, which is
517 shown in Fig. 8 (C). In this case, the stress results of the hydraulic pipeline are obtained in Fig. 8 (D),
518 where the maximum standard deviation of stress is 2.69×10^7 (Pa).

519 The goal of the optimization is to find the optimal locations of the pipeline hoops to minimize the
 520 maximum standard deviation of stress. Therefore, the objection function is $\sigma_{\sigma\max}$. In addition, the
 521 maximum standard deviation of displacement D_{\max} of the hydraulic pipeline is the constraint. The
 522 optimization problem of the hydraulic pipeline can be expressed as

$$\begin{aligned}
 & \text{Find } \mathbf{X}^* = \{X_1^*, X_2^*, \dots, X_{28}^*\} \\
 & \text{to minimize } \sigma_{\sigma\max} \\
 & \text{subject to } D_{\max} - D' < 0 \\
 & \quad X_i^l \leq X_i \leq X_i^u \quad (i = 1, 2, \dots, 28),
 \end{aligned} \tag{20}$$

523 where D' is the maximum standard deviation threshold value of displacement, which is set as
 524 5.5×10^{-4} . In other words, $D_{\max} < 5.5 \times 10^{-4}$ (m) must be satisfied in the whole optimization
 525 process. X_i^l and X_i^u are the lower and upper bounds of the design variable X_i , and are shown in
 526 Table 2. More detailed information on the maximum standard deviation of displacement D_{\max} of the
 527 aeronautical hydraulic pipeline can be found in (Wang et al. 2018).
 528

529 ***Sensitivity analysis and the optimization with variable screening***

530 The variable sensitivity results are obtained by the interval-based sensitivity index C_i , which are
 531 shown in Fig. 8 (E). It should be noted that the interval-based sensitivity analysis is performed based on
 532 a Kriging metamodel, which is built by 500 calls of the aeronautical hydraulic pipeline model in total.
 533 The specific procedure of the metamodel construction can be found in (Liu et al. 2018). In the
 534 application, the optimisation problem was required, by engineering designers, to have no more than 12
 535 design variables. According to Fig. 8 (E), ten most influential design variables can be selected, which
 536 are X_{24} , X_{14} , X_{13} , X_{12} , X_{19} , X_{15} , X_{25} , X_6 , X_{27} and X_3 , and other design variables have no or
 537 little effect on the maximum standard deviation of stress. Therefore, the 10 influential design variables
 538 are selected for the design optimization with variable screening (i.e., Top 10 optimization), which can
 539 be expressed as
 540

Find $X'_{\text{Top}} = \{X'_3, X'_6, X'_{12}, X'_{13}, X'_{14}, X'_{15}, X'_{19}, X'_{24}, X'_{25}, X'_{27}\}$

to minimize $\sigma_{\sigma_{\max}}(X_{\text{Top}}, X_{\sim\text{Top}})$

$$541 \quad \text{subject to } D_{\max} - D' < 0 \quad (21)$$

$$X_{\text{Top}}^l \leq X_{\text{Top}} \leq X_{\text{Top}}^u$$

$$X_{\sim \mathbf{Top}} = X_{\sim \mathbf{Top}}^{sv},$$

542 where $\mathbf{X}_{\sim \text{Top}}^{sv}$ is the selected specific value vector of the noninfluential variables $\mathbf{X}_{\sim \text{Top}}$, $\sigma_{\sigma_{\max}}$ and
 543 D_{\max} are directly obtained by the finite element model of the aeronautical hydraulic pipeline.

According to the interval-based sensitivity analysis, the noninfluential variables X_j ($j = 1, 2, 4, 5, 7 \sim 11, 16 \sim 18, 20 \sim 23, 26, 28$) are fixed as 34.84, 38.29, 45.51, 60.46, 16.03, 9.82, 10.72, 28.83, 12.10, 3.74, 2.63, 5.67, 37.45, 2.63, 5.68, 19.03, 1.88, 13.33, 1.23, 5.98, and 4.48, respectively. The optimization results of the traditional optimization method (i.e., all-variable optimization or the Top 28 optimization) and the optimization results with variable screening (i.e., the Top 10 optimization) are shown in Fig. 8 (F). The SQP optimizer is employed for the aeronautical hydraulic pipeline optimization. The optimized maximum standard deviation stress of the Top 28 is 2.42×10^7 (Pa) (shown in the right contour results of Fig. 8 (F)), while the optimized maximum standard deviation stress of the Top 10 is 2.43×10^7 (Pa) (shown in the left contour results of Fig. 8 (F)). It should be noted that the Top 10 optimization converges after 181 iterations, while the Top 28 optimization does not converge until the maximum allowable iterations (i.e., 550).

555

Discussions about the results

557 By comparing the optimization history of the Top 28 optimization and the Top 10 optimization
 558 (shown in Fig. 8 (F)), it is evident that the optimal result (2.42×10^7 (Pa)) of the Top 28 optimization
 559 is almost equal to the optimal result (2.43×10^7 (Pa)) of the Top 10 optimization, indicating that the
 560 eliminated 18 design variables have little effect on the maximum standard deviation of stress of the
 561 hydraulic pipeline. Therefore, the interval-based sensitivity index C_i is effective to identify these
 562 influential design variables and eliminate the remaining noninfluential design variables. The calculation
 563 cost for SQP optimizer has been reduced from 550 iterations to 181 iterations during the optimization,

564 which is a decrease of 68%. It is worth noting that, although variable selection by sensitivity analysis
565 incurs additional computational cost, engineers do not use the optimization model only once, but rather
566 use it repeatedly throughout subsequent analyses of the product. Furthermore, for some complex
567 engineering problems, the result of Top m optimization may be better than the result of the optimization
568 with all variables (Wang et al. 2018). In addition, it should be noted that when the concerned model is a
569 complex engineering problem without explicit performance function, such as the aeronautical hydraulic
570 pipelines in this work, the calculation of sensitivity indices (including Sobol' indices, Wang's indices,
571 and the interval-based sensitivity index) is time-consuming. In this case, the multi-fidelity surrogate
572 model (Alemazkoor et al. 2022; Meng et al. 2021) may be a suitable choice. First, the sensitivity
573 indices are obtained by a low-fidelity surrogate model. Then, the high-fidelity finite element model is
574 used for the optimization.

575 As can be seen, in the high-dimensional optimization problem, eliminating those noninfluential
576 design variables can greatly simplify the optimisation problem, and at the same time, relatively
577 adequate results can also be obtained. Ultimately, engineers can use the simplified models (rather than
578 the original high-dimensional complex models) in their subsequent work.

579

580 Conclusion

581 This paper introduces the interval-based sensitivity index and shows how the sensitivity analysis
582 can be used for solving high-dimensional optimization problems. Based on the introduction of the
583 interval field, the interval-based sensitivity index is reviewed and compared with other existing indices
584 by an illustrative function. The screening procedure based on this sensitivity index is applied to
585 high-dimensional design optimization problems involving two illustrative optimization examples and
586 an aeronautical hydraulic pipeline. The results show that the interval-based sensitivity index can
587 provide comprehensive effect information of input variables to the model output, thus effectively
588 screening out influential variables to remodel the high-dimensional optimization problems and
589 providing the guidance for the determination/realization of value-fixation of noninfluential variables.

590 Moreover, compared with Sobol' and Wang's indices, the interval-based sensitivity index is easy to use
 591 and has a superior performance.

592 It should be noted that the interval-based sensitivity analysis remains largely unexplored, and
 593 related studies are still rare. This paper explores a theoretical foundation for design optimization with
 594 variable screening by interval-based sensitivity analysis. It is admitted that sensitivity analysis is
 595 time-consuming, especially when the concerned models is a complex engineering problem. The
 596 interval-based sensitivity index is heuristic and more efficient computing strategies for evaluating this
 597 index will be further explored.

598 In this work, we focus on the single-objective optimization problem where we only need to
 599 evaluate the variable importance to a single model output. An important and practical perspective is to
 600 investigate the application of the proposed approach to multi-objective optimization problems by
 601 extending the interval sensitivity index. At the same time, the interval sensitivity index can also be
 602 extended to time-dependent reliability-based design optimization problems.

603

604 **Appendix A: Extension of the interval sensitivity index to consider the joint effect**
 605 **of two or more input variables**

606 The case of two variables (X_i and X_j) is derived as (Chang et al. 2022)

$$\begin{aligned}
 C_{ij} &= \frac{D_u(ij) + D_l(ij)}{D_{total}(ij)} \\
 &= \frac{D_{total}(ij) - D_{NIP}(ij)}{D_{total}(ij)} = 1 - \frac{D_{NIP}(ij)}{D_{total}(ij)} \\
 &= 1 - \frac{1}{4(Y^u - Y^l)} \int_{-1}^1 \int_{-1}^1 (g^u(\delta_i, \delta_j) - g^l(\delta_i, \delta_j)) d\delta_i d\delta_j \\
 &= 1 - \frac{1}{2(Y^u - Y^l)} \int_{-1}^1 \int_{-1}^1 g^r(\delta_i, \delta_j) d\delta_i d\delta_j
 \end{aligned} \tag{A22}$$

608 and the case of m variables (X_i, X_j, \dots, X_k) is derived by the following expression (Chang et al.
 609 2022):

$$\begin{aligned}
C_{\underbrace{ij \cdots k}_m} &= \frac{D_u(ij \cdots k) + D_l(ij \cdots k)}{D_{total}(ij \cdots k)} \\
&= \frac{D_{total} - D_{NIP}(ij \cdots k)}{D_{total}(ij \cdots k)} = 1 - \frac{D_{NIP}(ij \cdots k)}{D_{total}(ij \cdots k)} \\
610 \quad &= 1 - \frac{1}{2^m (Y^u - Y^l)} \int_{-1}^1 \cdots \int_{-1}^1 (g^u(\delta_i, \delta_j, \cdots, \delta_k) - g^l(\delta_i, \delta_j, \cdots, \delta_k)) d\delta_i d\delta_j \cdots d\delta_k \\
&= 1 - \frac{1}{2^{m-1} (Y^u - Y^l)} \int_{-1}^1 \cdots \int_{-1}^1 g^r(\delta_i, \delta_j, \cdots, \delta_k) d\delta_i d\delta_j \cdots d\delta_k,
\end{aligned} \tag{A23}$$

611 where $D(ij)$ indicates a two-dimensional domain and $D(ij \cdots k)$ indicates a m -dimensional domain.

612 It should be noted that g indicates interval fields in Eqs. (A1) and (A2).

613

614 Appendix B: Review of Sobol' indices

615 For a model $Y = f(\mathbf{X})$ where all elements of \mathbf{X} are independent, the variance decomposition
616 of the model response Y can be expressed as (Homma and Saltelli 1996; Sobol' 1993; Sobol' 2001)

$$617 \quad V_Y = \sum_i V_i + \sum_i \sum_{j>i} V_{ij} + \cdots + V_{12 \cdots n}, \tag{B1}$$

618 where $V_i = \text{Var}[\mathbb{E}(Y|X_i)]$ and $V_{ij} = \text{Var}[\mathbb{E}(Y|X_i, X_j)] - V_i - V_j$. Dividing both sides of Eq. (B1)
619 by V_Y yields:

$$620 \quad 1 = \sum_i S_i + \sum_i \sum_{j>i} S_{ij} + \cdots + S_{12 \cdots n}, \tag{B2}$$

621 where $S_i = V_i / V_Y$ is the main effect index of X_i and $S_{ij} = V_{ij} / V_Y$ is the second order effect
622 between X_i and X_j . Finally, the total effect index S_{Ti} is defined as (Homma and Saltelli 1996)

$$623 \quad S_{Ti} = S_i + \sum_{i \neq j} S_{ij} + \cdots + S_{12 \cdots n} = \frac{\mathbb{E}[\text{Var}(Y|X_{-i})]}{V_Y} = \frac{V_{Ti}}{V_Y}. \tag{B3}$$

624 The main index S_i and total index S_{Ti} are often used to measure the importance of each random
625 input. $S_i > S_j$ indicates that X_i is more important than X_j in the sense of individual contribution
626 to the model output variance. Similarly, $S_{Ti} > S_{Tj}$ indicates that X_i contributes more to the model
627 output variance than X_j . It should be noted that the total effect index S_{Ti} is usually used when
628 screening the influential variables (Cho et al. 2014; Wei et al. 2015). A more detailed description can be
629 found in (Homma and Saltelli 1996; Sobol' 1993; Sobol' 2001; Wei et al. 2015).

630

631 **Appendix C: Review of Wang's indices**

632 For a model $Y = f(\mathbf{X})$, the input variables \mathbf{X} are intervals and the output Y is also an
 633 interval, i.e., $Y \in Y' = [Y', Y'']$ where Y' and Y'' are the lower and upper bounds of Y' . Its centre
 634 value and radius can be defined as $Y^c = (Y'' + Y')/2$ and $Y^r = (Y'' - Y')/2$, respectively. Then, the
 635 centre value Y^c and radius Y^r can be combined into the following form (Guo and Lu 2015; Guo and
 636 Lu 2001):

637
$$\eta = \frac{Y^c}{Y^r}. \quad (C1)$$

638 When X_i is fixed at a specific value in its interval, the impact of the uncertainty of X_i on η
 639 will be eliminated. If X_i takes different values in its interval, η will also be an interval that can be
 640 expressed as $\eta|X_i$. The lower and upper bounds of $\eta|X_i$ can be expressed as

641
$$[\eta|X_i]^l = \min_{X_i \in [X_i', X_i'']} \eta|X_i \quad (C2)$$

642 and

643
$$[\eta|X_i]^u = \max_{X_i \in [X_i', X_i'']} \eta|X_i. \quad (C3)$$

644 The centre value and radius of $\eta|X_i$ are given as

645
$$[\eta|X_i]^c = \frac{[\eta|X_i]^u + [\eta|X_i]^l}{2} \quad (C4)$$

646 and

647
$$[\eta|X_i]^r = \frac{[\eta|X_i]^u - [\eta|X_i]^l}{2}. \quad (C5)$$

648 Finally, two non-probabilistic sensitivity indices (centre value sensitivity ζ and radius sensitivity ς)
 649 can be expressed as (Li et al. 2013; Wang et al. 2018)

650
$$\zeta_i = \frac{|\eta - [\eta|X_i]^c|}{\eta} \quad (C6)$$

651 and

652
$$\varsigma_i = \frac{[\eta|X_i]^r}{\eta}. \quad (C7)$$

653 Wang's two sensitivity indices quantify the effect of the interval variables on η (which is
 654 combined by centre value Y^c and radius Y^r of model output Y) from the perspective of the centre
 655 value and radius, respectively. A detailed description of Wang's indices can be found in (Wang et al.
 656 2018). In addition, it should be pointed out that Wang's two sensitivity indices described in Eqs.

657 (C2-C7) have the same form and definition as Li's importance measures (Li et al. 2013), although Li's
658 measures are concerned with a non-probabilistic reliability index rather than system output response.

659

660 **Data Availability Statement**

661 All data, models, or code that support the findings of this study are available from the
662 corresponding author upon reasonable request.

663

664 **Acknowledgment**

665 This work is supported by the National Natural Science Foundation of China (Grant No.
666 NSFC51975476). The first author is sponsored by Innovation Foundation for Doctor Dissertation of
667 Northwestern Polytechnical University (Grant No. CX2022012).

668

669 **References**

670 Alemazkoor, N., A. Louhghalam, and M. Tootkaboni. 2022. "A multi-fidelity polynomial chaos-greedy
671 Kaczmarz approach for resource-efficient uncertainty quantification on limited budget." *Computer Methods in Applied Mechanics and Engineering*, 389: 114290.

672 Arwade, S. R., M. Moradi, and A. Louhghalam. 2010. "Variance decomposition and global sensitivity
673 for structural systems." *Engineering Structures*, 32 (1): 1–10.

674 Borgonovo, E. 2007. "A new uncertainty importance measure." *Reliability Engineering and System
675 Safety*, 92 (6): 771–784.

676 Borgonovo, E., and E. Plischke. 2016. "Sensitivity analysis: a review of recent advances." *European
677 Journal of Operational Research*, 248 (3): 869–887.

678 Breiman, L. 2001. "Random forests." *Machine Learning*, 45 (1): 5–32.

680 Chang, Q., C. Zhou, P. Wei, Y. Zhang, and Z. Yue. 2021. "A new non-probabilistic time-dependent
681 reliability model for mechanisms with interval uncertainties." *Reliability Engineering and System
682 Safety*, 215: 107771.

683 Chang, Q., C. Zhou, M. A. Valdebenito, H. Liu, and Z. Yue. 2022. “A novel sensitivity index for
684 analyzing the response of numerical models with interval inputs.” *Computer Methods in Applied*
685 *Mechanics and Engineering*, 400: 115509.

686 Cho, H., S. Bae, K. K. Choi, D. Lamb, and R. J. Yang. 2014. “An efficient variable screening method
687 for effective surrogate models for reliability-based design optimization.” *Structural and*
688 *Multidisciplinary Optimization*, 50 (5): 717–738.

689 Constantine, P. G., E. Dow, and Q. Wang. 2013. “Active subspace methods in theory and practice:
690 applications to kriging surfaces.” *SIAM Journal on Scientific Computing*, 36(4), 1500–1524.

691 Craig, K. J., N. Stander, D. A. Dooge, and S. Varadappa. 2005. “Automotive crashworthiness design
692 using response surface-based variable screening and optimization.” *Engineering Computations*,
693 22 (1): 38–61.

694 Duarte Silva, A. P. 2001. “Efficient variable screening for multivariate analysis.” *Journal of*
695 *Multivariate Analysis*, 76 (1): 35–62.

696 Faes, M., J. Cerneels, D. Vandepitte, and D. Moens. 2017. “Identification and quantification of
697 multivariate interval uncertainty in finite element models.” *Computer Methods in Applied*
698 *Mechanics and Engineering*, 315: 896–920.

699 Faes, M., and D. Moens. 2020. “Recent trends in the modeling and quantification of non-probabilistic
700 uncertainty.” *Archives of Computational Methods in Engineering*, 27, 633–671.

701 Fesanghary, M., E. Damangir, and I. Soleimani. 2009. “Design optimization of shell and tube heat
702 exchangers using global sensitivity analysis and harmony search algorithm.” *Applied Thermal*
703 *Engineering*, 29 (5–6): 1026–1031.

704 Fort, J. C., T. Klein, and N. Rachdi. 2016. “New sensitivity analysis subordinated to a contrast.”
705 *Communications in Statistics-Theory and Methods*, 45 (15): 4349–4364.

706 Fu, G., Z. Kapelan, and P. Reed. 2012. “Reducing the complexity of multiobjective water distribution
707 system optimization through global sensitivity analysis.” *Journal of Water Resources Planning*
708 *and Management*, 138 (3): 196–207.

709 Gao, B., Y. Ren, H. Jiang, and J. Xiang. 2019. “Sensitivity analysis-based variable screening and
710 reliability optimisation for composite fuselage frame crashworthiness design.” *International
711 Journal of Crashworthiness*, 24 (4): 380–388.

712 Guo, S. X., and Z. Z. Lu. 2015. “A non-probabilistic robust reliability method for analysis and design
713 optimization of structures with uncertain-but-bounded parameters.” *Applied Mathematical
714 Modelling*, 39(7), 1985–2002.

715 Guyon, I., and A. Elisseeff. 2003. “An introduction to variable and feature selection.” *Journal of
716 Machine Learning Research*, 3: 1157–1182.

717 Härdle, W., and L. Simar. 2003. “Applied multivariate statistical analysis.” *Springer Nature*.

718 Homma, T., and A. Saltelli. 1996. “Importance measures in global sensitivity analysis of nonlinear
719 models.” *Reliability Engineering and System Safety*, 52 (1): 1–17.

720 Jamian, J. J., M. N. Abdullah, H. Mokhlis, M. W. Mustafa, and A. H. A. Bakar. 2014. “Global particle
721 swarm optimization for high dimension numerical functions analysis.” *Journal of Applied
722 Mathematics*, 36(2): 329193

723 Jiang, C., B. Y. Ni, X. Han, and Y. R. Tao. 2014. “Non-probabilistic convex model process: A new
724 method of time-variant uncertainty analysis and its application to structural dynamic reliability
725 problems.” *Computer Methods in Applied Mechanics and Engineering*, 268: 656–676.

726 Jolliffe, I. T. 2002. “Principal component analysis.” *Journal of Marketing Research*, 87 (4): 513.

727 Li, G., Z. Lu, L. Tian, and J. Xu. 2013. “The importance measure on the non-probabilistic reliability
728 index of uncertain structures.” *Proceedings of the Institution of Mechanical Engineers, Part O:
729 Journal of Risk and Reliability*, 227 (6): 651–661.

730 Li, J., Q. Y. Duan, W. Gong, A. Ye, Y. Dai, C. Miao, Z. Di, C. Tong, and Y. Sun. 2013b. “Assessing
731 parameter importance of the common land model based on qualitative and quantitative sensitivity
732 analysis.” *Hydrology and Earth System Sciences*, 17 (8): 3279–3293.

733 Li, L., Q. Chang, C. Zhou, W. Wang, and Z. Zhang. 2020. “Sensitivity analysis-based optimization: a
734 case study with the MTBF of an aeronautical hydraulic pipeline system.” *International Journal of*

761 optimization of multi-motor driving transmission system.” *Structural and Multidisciplinary*
762 *Optimization*, 58 (2): 797–816.

763 Sobol’, I. M. 1993. “Sensitivity analysis for non-linear mathematical models.” *Mathematical Modeling*
764 *and Computational Experiment*, 1: 407-414.

765 Sobol’, I. M., and S. Kucherenko. 2009. “Derivative based global sensitivity measures and their link
766 with global sensitivity indices.” *Mathematics and Computers in Simulation*, 79 (10): 3009–3017.

767 Sobol’, I. M. 2001. “Global sensitivity indices for nonlinear mathematical models and their Monte
768 Carlo estimates.” *Mathematics and Computers in Simulation*, 55 (1): 271–280.

769 Spagnol, A., R. Le Riche, and S. Da Veiga. 2019. “Global sensitivity analysis for optimization with
770 variable selection.” *SIAM-ASA Journal on Uncertainty Quantification*, 7 (2): 417–443.

771 Tang, Z., Z. Lu, D. Li, and F. Zhang. 2011. “Optimal design of the positions of the hoops for a
772 hydraulic pipelines system.” *Nuclear Engineering and Design*, 241 (12): 4840–4855.

773 Tian, W., C. Jiang, B. Ni, Z. Wu, Q. Wang, and L. Yang. 2018. “Global sensitivity analysis and
774 multi-objective optimization design of temperature field of sinter cooler based on energy value.”
775 *Applied Thermal Engineering*, 143: 759–766.

776 Valdebenito, M. A., and G. I. Schuëller. 2010. “A survey on approaches for reliability-based
777 optimization.” *Structural and Multidisciplinary Optimization*, 42 (5): 645–663.

778 Wang, L., D. Liu, Y. Yang, and J. Hu. 2019. “Novel methodology of non-probabilistic reliability-based
779 topology optimization (NRBTO) for multi-material layout design via interval and convex mixed
780 uncertainties.” *Computer Methods in Applied Mechanics and Engineering*, 346: 550–573.

781 Wang, L., Y. Liu, D. Liu, and Z. Wu. 2021. “A novel dynamic reliability-based topology optimization
782 (DRBTO) framework for continuum structures via interval-process collocation and the
783 first-passage theories.” *Computer Methods in Applied Mechanics and Engineering*, 386: 114107.

784 Wang, W., C. Zhou, H. Gao, and Z. Zhang. 2018. “Application of non-probabilistic sensitivity analysis
785 in the optimization of aeronautical hydraulic pipelines.” *Structural and Multidisciplinary*
786 *Optimization*, 57 (6): 2177–2191.

787 Wang, Y., and C. A. Shoemaker. 2014. “A general stochastic algorithmic framework for minimizing
788 expensive black box objective functions based on surrogate models and sensitivity analysis.”
789 *arXiv preprint*, arXiv:1410.6271.

790 Wei, P., Z. Lu, and J. Song. 2015a. “Variable importance analysis: a comprehensive review.”
791 *Reliability Engineering and System Safety*, 142: 399–432.

792 Wei, P., Z. Lu, and J. Song. 2015. “A comprehensive comparison of two variable importance analysis
793 techniques in high dimensions: application to an environmental multi-indicators system.”
794 *Environmental Modelling and Software*, 70: 178–190.

795 Welch, W. J., R. J. Buck, J. Sacks, H. P. Wynn, T. J. Mitchell, and M. D. Morris. 1992. “Screening,
796 predicting, and computer experiments.” *Technometrics*, 34 (1): 15–25.

797 Wu, J., O. Sigmund, and J. P. Groen. 2021. “Topology optimization of multi-scale structures: a
798 review.” *Structural and Multidisciplinary Optimization*, 63 (3): 1455–1480.

799 Zhang, Y., X. Zhang, P. Huang, and Y. Sun. 2020. “Global sensitivity analysis for key parameters
800 identification of net-zero energy buildings for grid interaction optimization.” *Applied Energy*,
801 279: 115820.

802 Zhang, Z., C. Zhou, W. Wang, and Z. Yue. 2019. “Optimization design of aeronautical hydraulic
803 pipeline system based on non-probabilistic sensitivity analysis.” *Proceedings of the Institution of
804 Mechanical Engineers, Part O: Journal of Risk and Reliability*, 233 (5): 815–825.

805 Zhou, C., Q. Chang, H. Zhao, M. Ji, and Z. Shi. 2021. “Fault tree analysis with interval uncertainty: a
806 case study of the aircraft flap mechanism.” *IEEE Transactions on Reliability*, 70 (3): 944–956.

807 Zhou, C., Z. Zhang, F. Liu, and W. Wang. 2019. “Sensitivity analysis for probabilistic anti-resonance
808 design of aeronautical hydraulic pipelines.” *Chinese Journal of Aeronautics*, 32 (4): 948–953.

809

Table 1 Two cases for the four-variable function with corresponding inputs and outputs

	\mathbf{X}^l	\mathbf{X}^u	$f^l(\mathbf{X})$	$f^u(\mathbf{X})$	$f^c(\mathbf{X})$	$f^r(\mathbf{X})$
Case 1	(5, 5, 5, 5,)	(6, 6, 6, 6)	2450	5112	3781	1331
Case 2	(-0.5, -0.5, -0.5, -0.5)	(0.5, 0.5, 0.5, 0.5)	-2.25	2.75	0.25	2.5

Algorithm 1 Pseudocode of the strategy to calculate the interval-based sensitivity index C_i

- 1 Generate initial points $\{\delta_{i(1)}, \dots, \delta_{i(n_m)}\}$
- 2 Call surrogate optimisation algorithm
- 3 Obtain the corresponding lower/upper bounds $\{g^l(\delta_{i(1)}), \dots, g^l(\delta_{i(n_m)})\}/\{g^u(\delta_{i(1)}), \dots, g^u(\delta_{i(n_m)})\}$
- 4 Use the training data set to construct a metamodel of $g^l(\delta_i)/g^u(\delta_i)$
- 5 **While** $n_{ini} + n_{new} < n_e$ or $\max \hat{\sigma}^2(\delta_i) > \sigma_e^2$
 - % $n_{ini} + n_{new}$ is the total number of model calls
 - % $\max \hat{\sigma}^2(\delta_i)$ is the maximum of mean square error
- 6 Use an adaptive sampling criterion to sample a new point $\delta_{i(new)}$
- 7 Call surrogate optimisation algorithm
- 8 Obtain its corresponding lower/upper bound $g^l(\delta_{i(new)})/g^u(\delta_{i(new)})$
- 9 Update training data set by involving $\delta_{i(new)}$ and $g^l(\delta_{i(new)})/g^u(\delta_{i(new)})$ respectively
- 10 **End While**
- 11 Export final metamodels of the lower/upper bound $g^l(\delta_i)/g^u(\delta_i)$
- 12 The final metamodels $g^l(\delta_i)$ and $g^u(\delta_i)$ are used to obtain $A_{NIP}(i)$
- 13 $C_i = 1 - A_{NIP}(i)/A_{total}$

Table 2 Section of input variables and their initial value, lower bounds, and upper bounds.

Variables	X_1	X_2	X_3	X_4	X_5	X_6	X_7	X_8	X_9	X_{10}	X_{11}	X_{12}	X_{13}	X_{14}
Position	14 ^X	17 ^X	20 ^X	23 ^X	26 ^X	30 ^X	33 ^X	36 ^X	39 ^X	40 ^X	42 ^X	45 ^X	45 ^Z	51 ^X
X^0 (mm)	43	35	93	55	56	110	158	88	93	290	117	30	30	67
X^l (mm)	34	28	72	43	47	97	147	68	78	287	111	25	25	53
X^u (mm)	52	42	114	67	65	123	169	108	108	293	123	35	35	81
Variables	X_{15}	X_{16}	X_{17}	X_{18}	X_{19}	X_{20}	X_{21}	X_{22}	X_{23}	X_{24}	X_{25}	X_{26}	X_{27}	X_{28}
Position	54 ^X	59 ^X	62 ^X	62 ^Y	65 ^X	69 ^X	69 ^Y	72 ^X	72 ^Y	75 ^X	75 ^Y	82 ^X	82 ^Y	82 ^Z
X^0 (mm)	63	36	29	59	56	187	20	111	13	78	7	54	28	50
X^l (mm)	53	29	26	48	50	183	18	88	12	61	5	43	25	40
X^u (mm)	73	43	32	70	62	191	22	134	14	95	9	65	31	60

* The superscript X, Y and Z of the position number are the coordinate of the hoops.

Fig 1

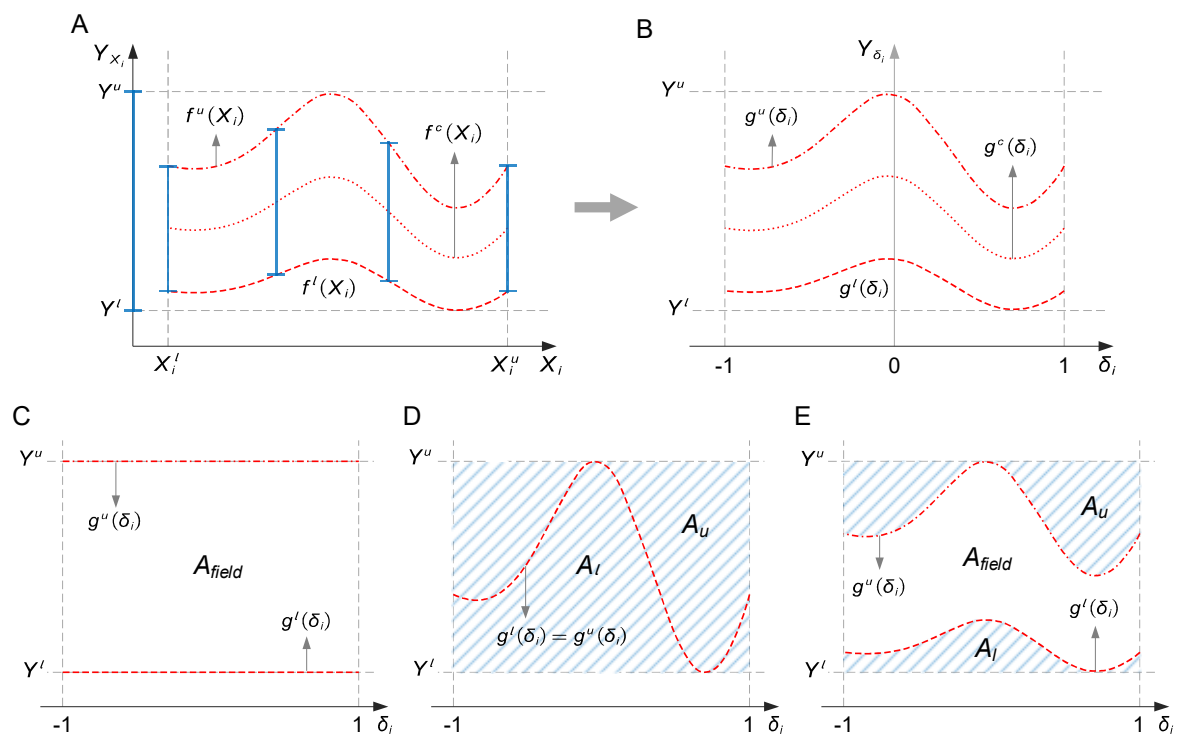


Fig 2

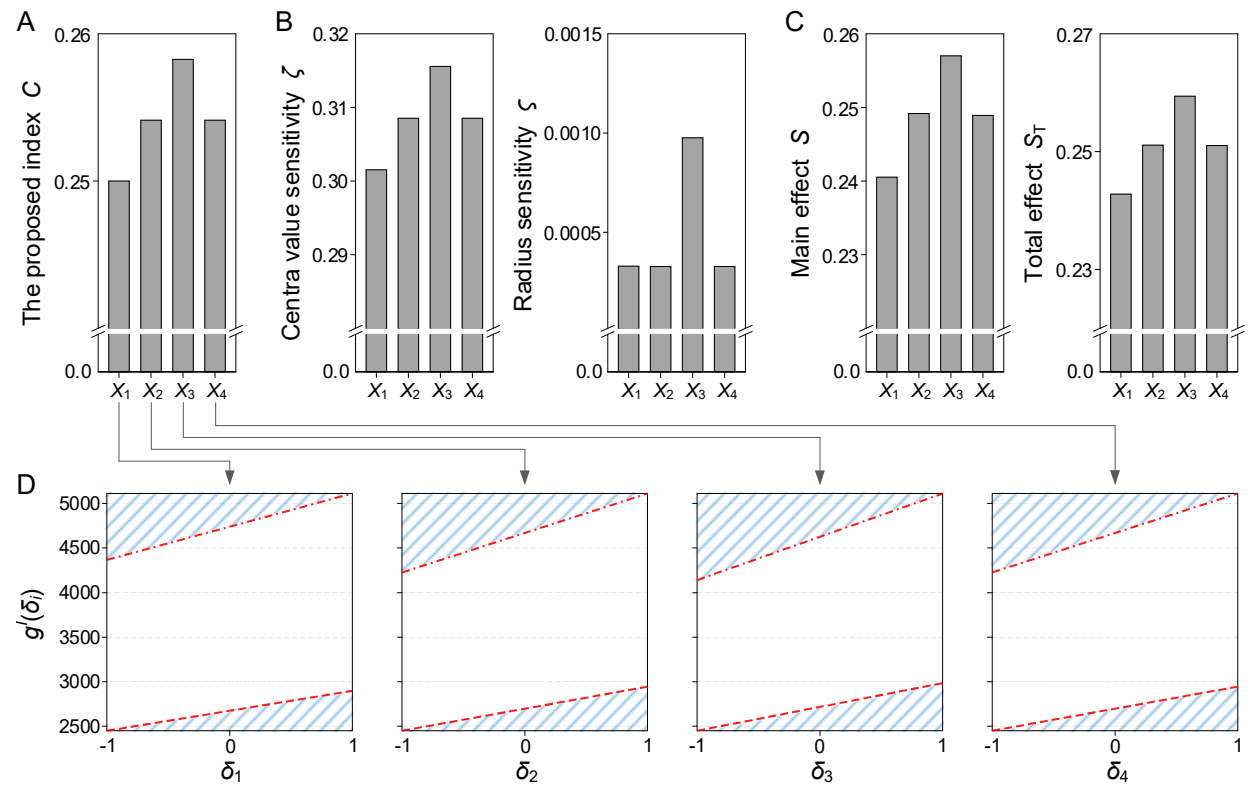


Fig 3

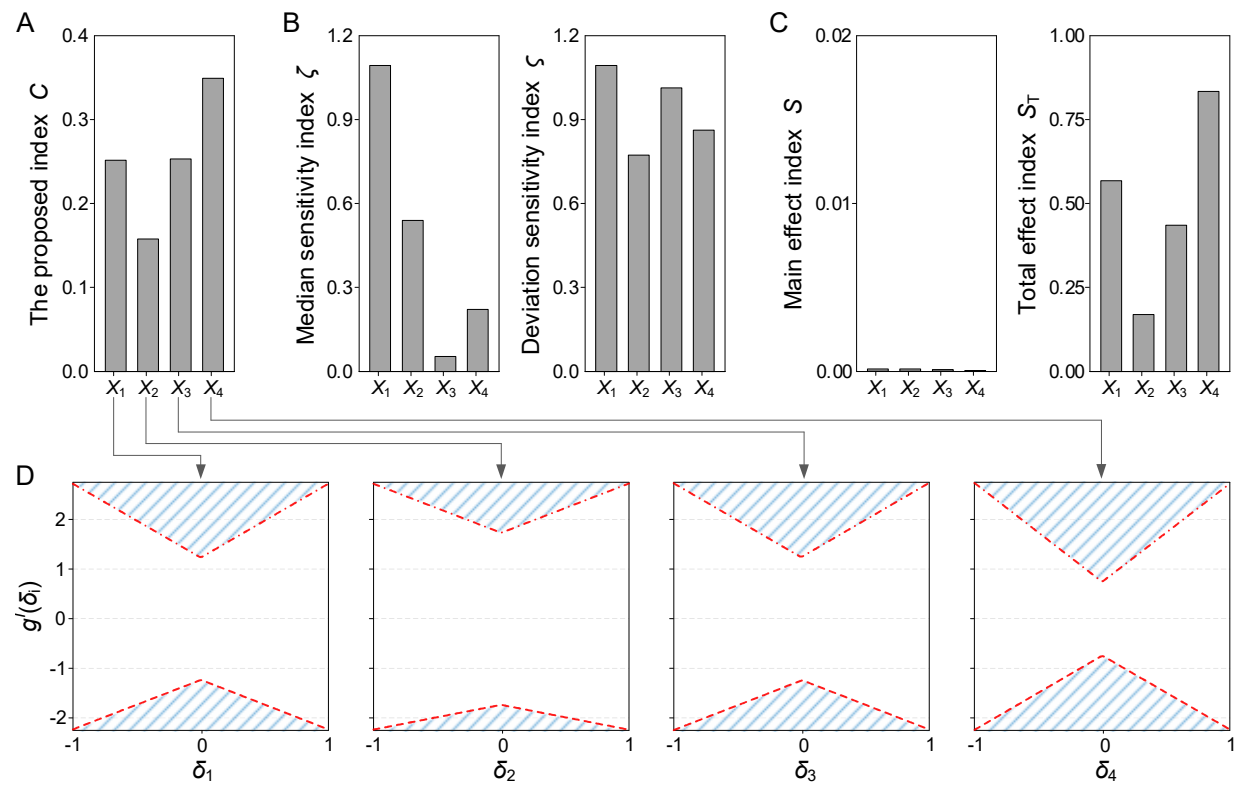


Fig 4

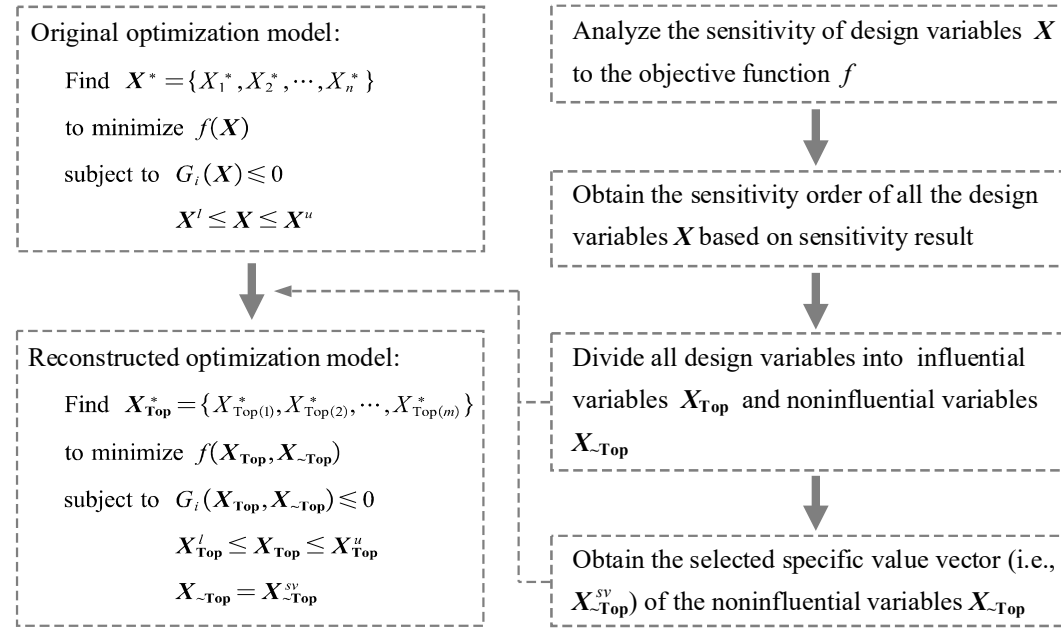
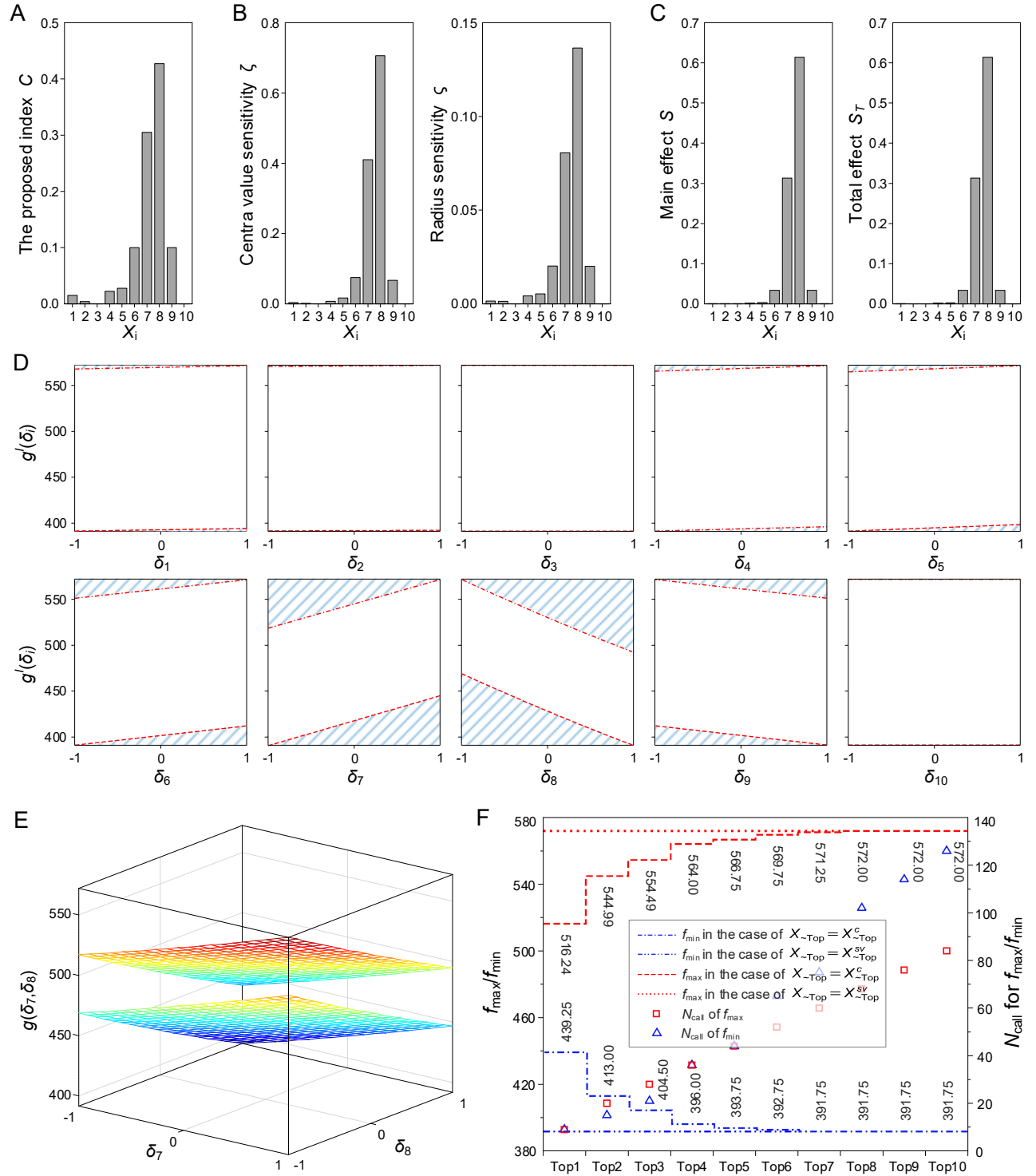


Fig 5



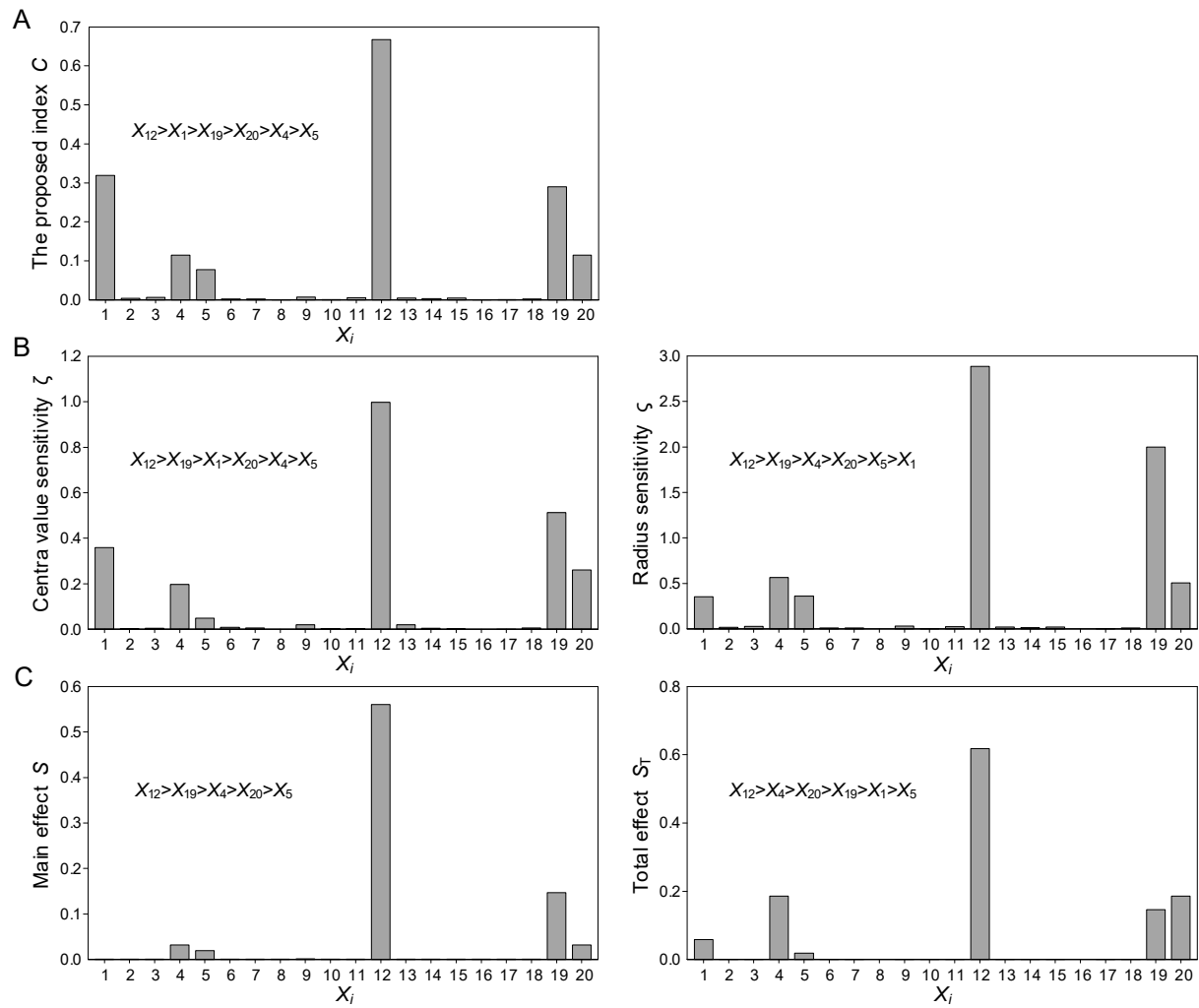
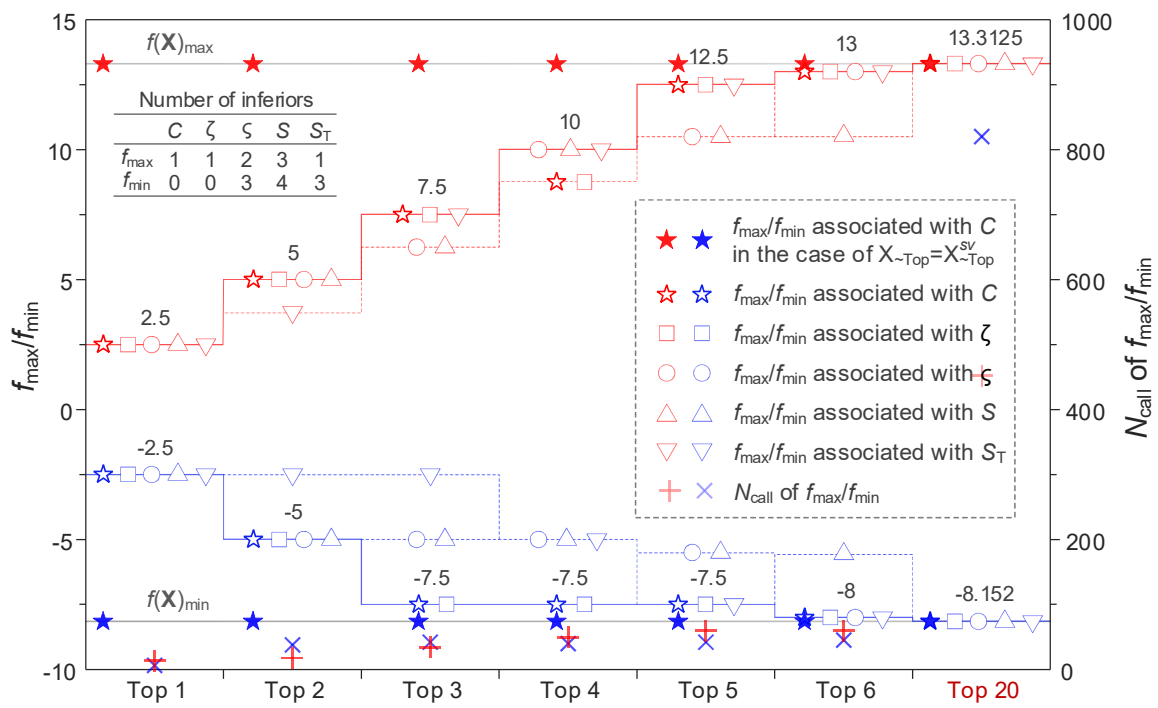


Fig 7



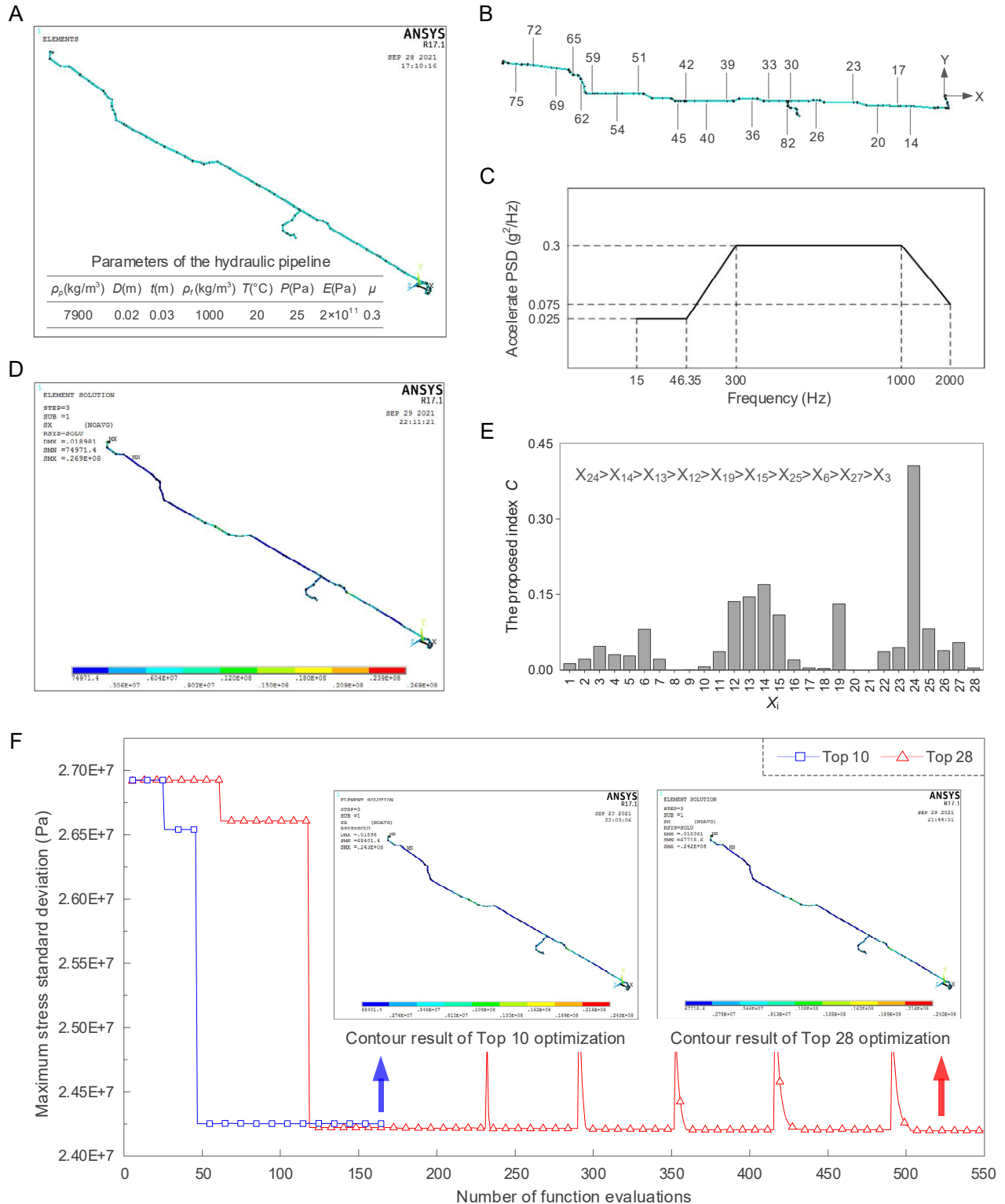


Fig. 1 Illustration of the interval field for variables: (A) is an interval field $f^I(X_i)$; (B) is a normalized interval field $g^I(\delta_i)$; (C) and (D) are two special interval field cases where the interval-based sensitivity index $C_i = 0$ and $C_i = 1$, respectively; (E) is a normalized interval field used to define the interval-based sensitivity index C_i .

Fig. 2 The sensitivity results in Case 1: (A) the interval-based sensitivity index C_i ; (B) Wang's indices; (C) Sobol' indices; (D) normalized interval fields to obtain C_1-C_4 .

Fig. 3 The sensitivity results in Case 2: (A) the interval-based sensitivity index C_i ; (B) Wang's indices; (C) Sobol' indices; (D) normalized interval fields to obtain C_1-C_4 .

Fig. 4 The general process of the design optimization with variable screening

Fig. 5 The sensitivity results and optimization results: (A) the interval-based sensitivity index C_i ; (B) Wang's indices; (C) Sobol' indices; (D) normalized interval field to obtain C_i ; (E) normalized interval field to obtain C_{78} ; (F) the maximum and minimum value (with its corresponding function calls) in the case of Top 1 to Top 10.

Fig. 6 The sensitivity results where (A) the interval-based sensitivity index C_i , (B) Wang's indices and (C) Sobol' indices

Fig. 7 The maximum and minimum values (with its corresponding function calls) obtained by three types of sensitivity indices (five indices in total) in the case of Top 1-6 and Top 20.

Fig. 8 Results of the aeronautical hydraulic pipeline where (A) shows the finite element model and its parameters; (B) node indices of hoops; (C) acceleration PSD function of stochastic excitation; (D) contour result of stress standard deviation before optimization; (E) the results of the interval-based sensitivity index; (F) the optimization history of maximum standard deviation of stress.